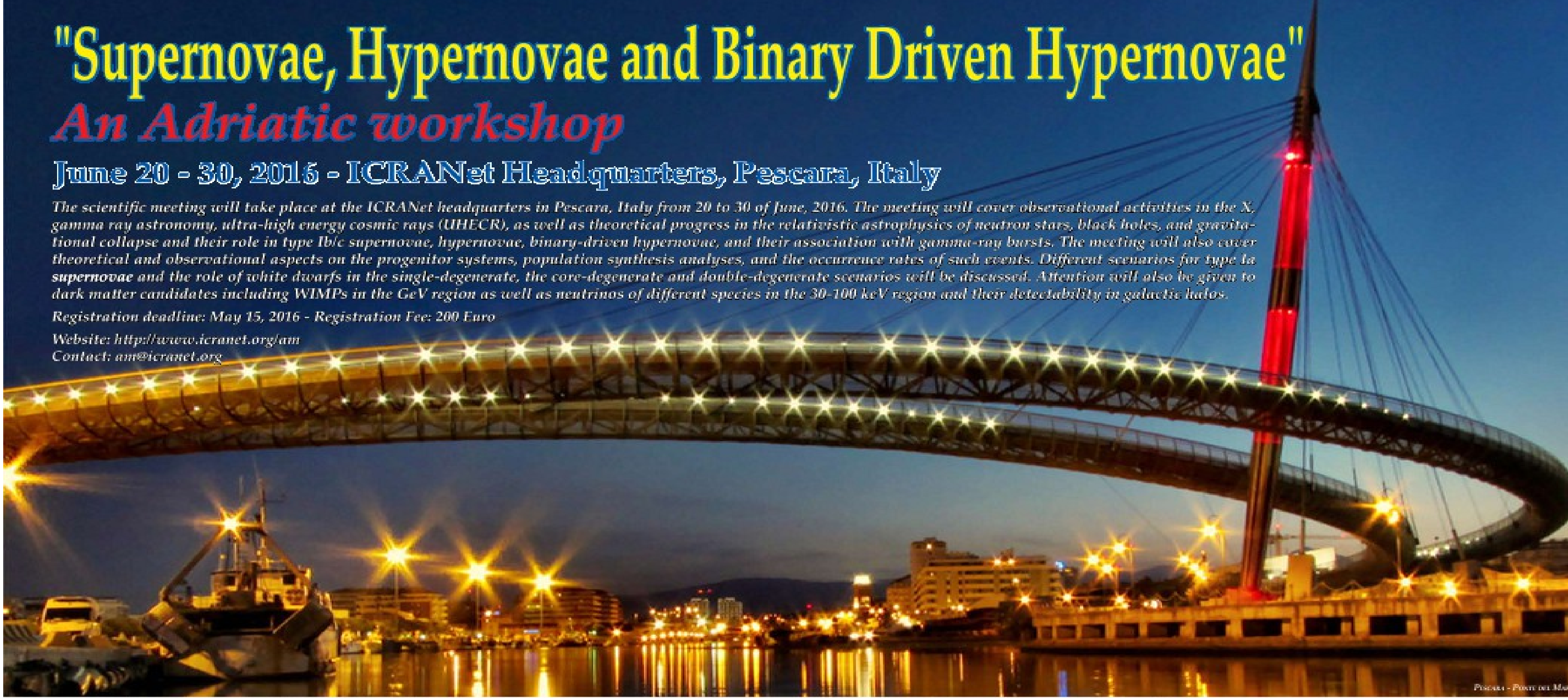

"Classification of long and short bursts and their rate of occurrence "

Marco Muccino

University of Rome “Sapienza” & ICRANet, Italy

On behalf of a large collaboration

R. Ruffini, Y. Aimuratov, L.M. Becerra, C.L. Bianco, M. Karlica, M. Kovacevic, R. Moradi, A.V. Penacchioni, G.B. Pisani, D. Primorac, J.A. Rueda and Y. Wang

Historical introduction

The discovery by the Vela satellites [1]

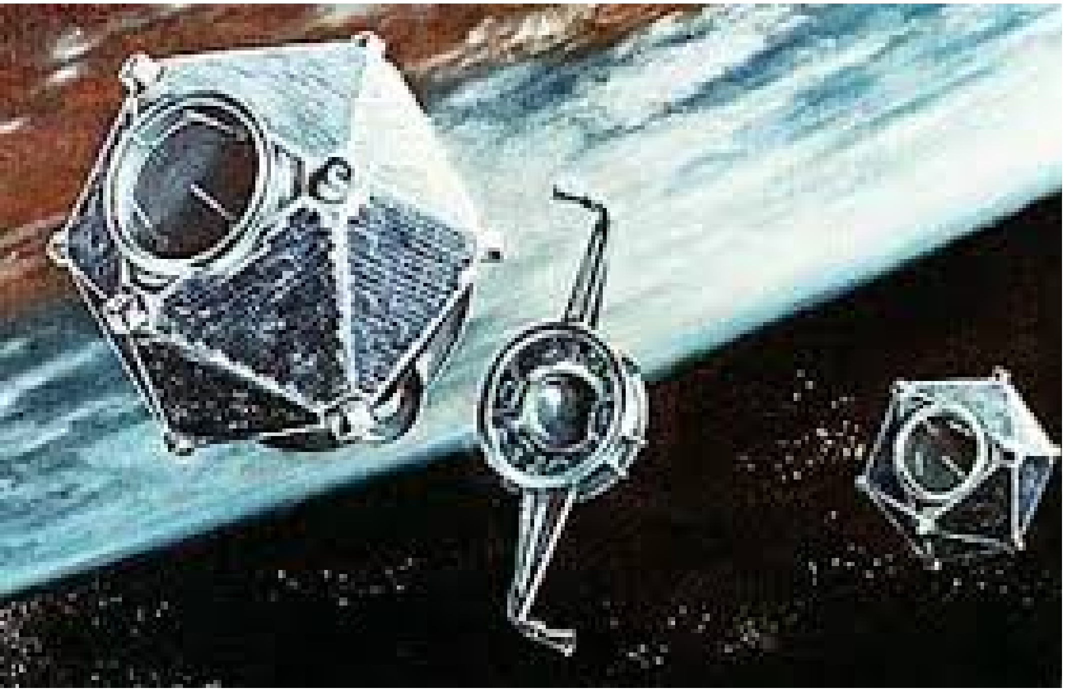

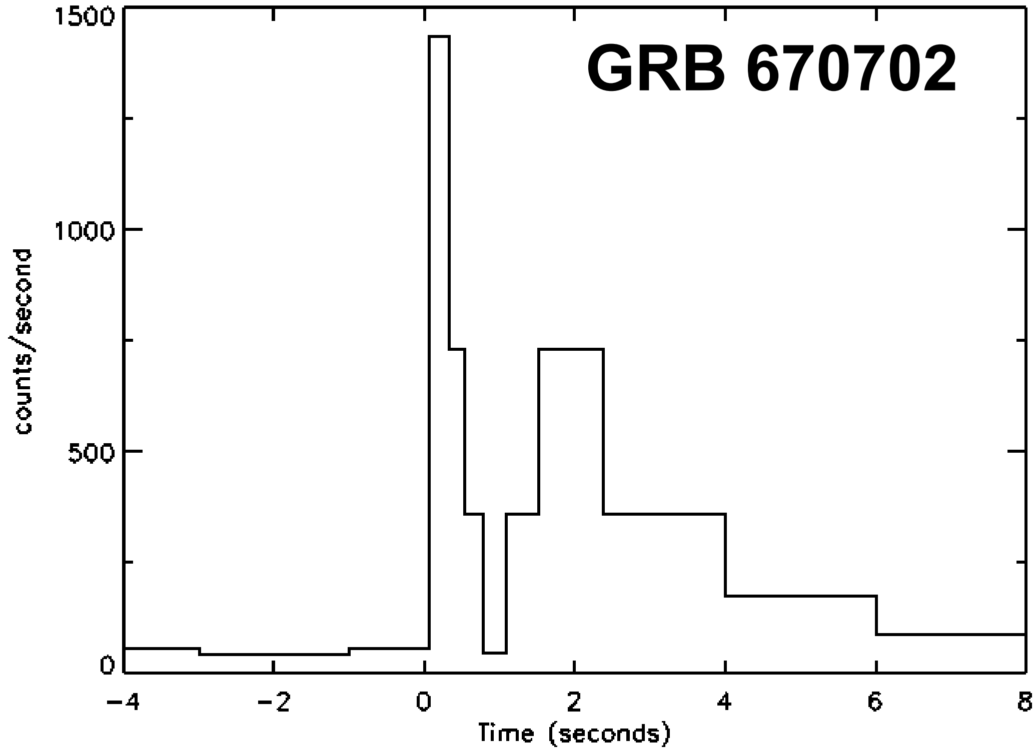

Already in 1974–1978 two general conclusions were advanced :

– the relation of GRBs with the “moment of gravitational collapse” leading to a BH formation [2];

– the role of an e^+e^- plasma for the origin of GRBs [3,4] at the very basis of the *fireshell model* and the *fireball model*.

[1] Strong, I. B., Klebesadel, R. W., & Evans, W. D. 1975, in Annals of the New York Academy of Sciences, Vol. 262, Seventh Texas Symposium on Relativistic Astrophysics, ed. P. G. Bergman, E. J. Fenyves, & L. Motz, 145–158

[2] Gursky, H., & Ruffini, R., eds. 1975, Astrophysics and Space Science Library, Vol. 48, Neutron stars, black holes and binary X-ray sources; Proceedings of the Annual Meeting, San Francisco, Calif., February 28, 1974

[3] Damour, T., & Ruffini, R. 1975, Physical Review Letters, 35, 463

[4] Cavallo, G., & Rees, M. J. 1978, MNRAS, 183, 359

The outcomes from the BATSE instrument [5]

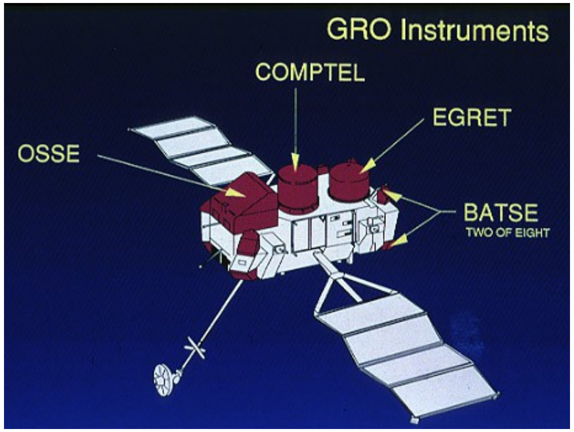

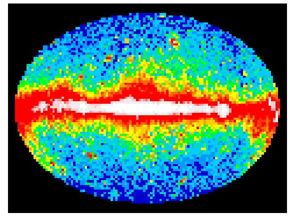

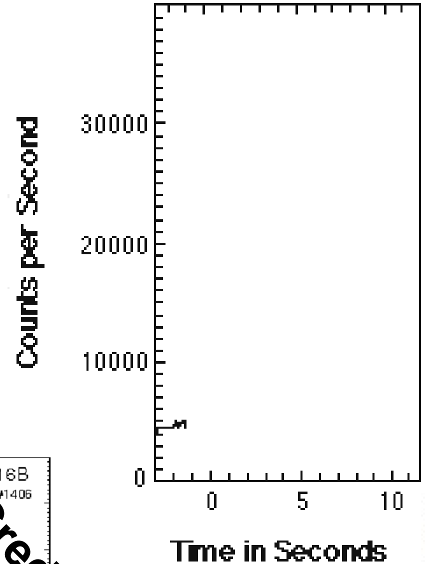

No concentration in the galactic plane pointing to the extragalactic origin.

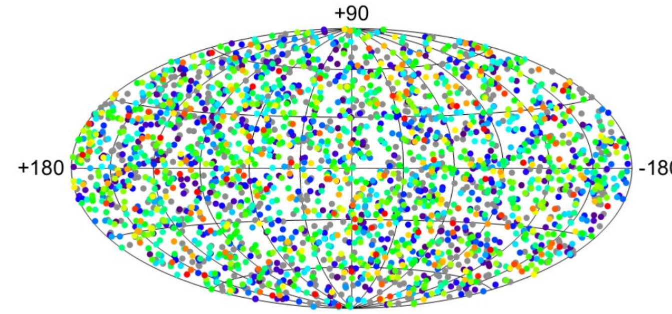

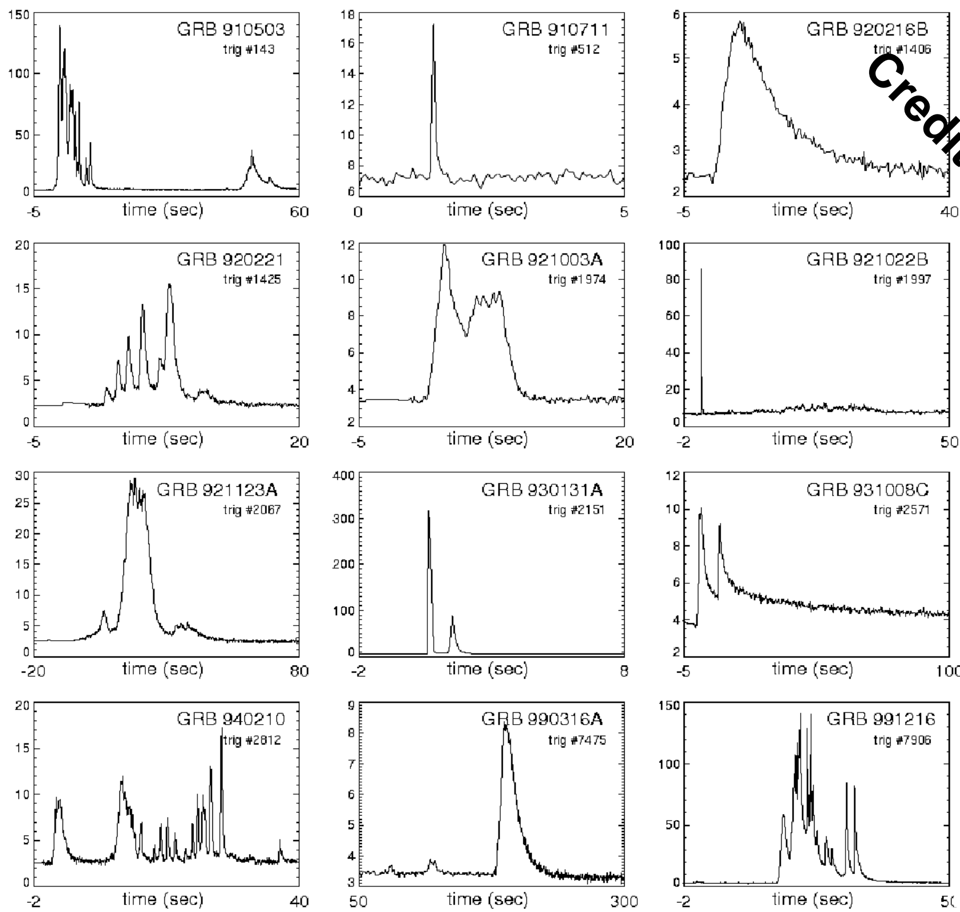

Credits: CGRO BATSE Team

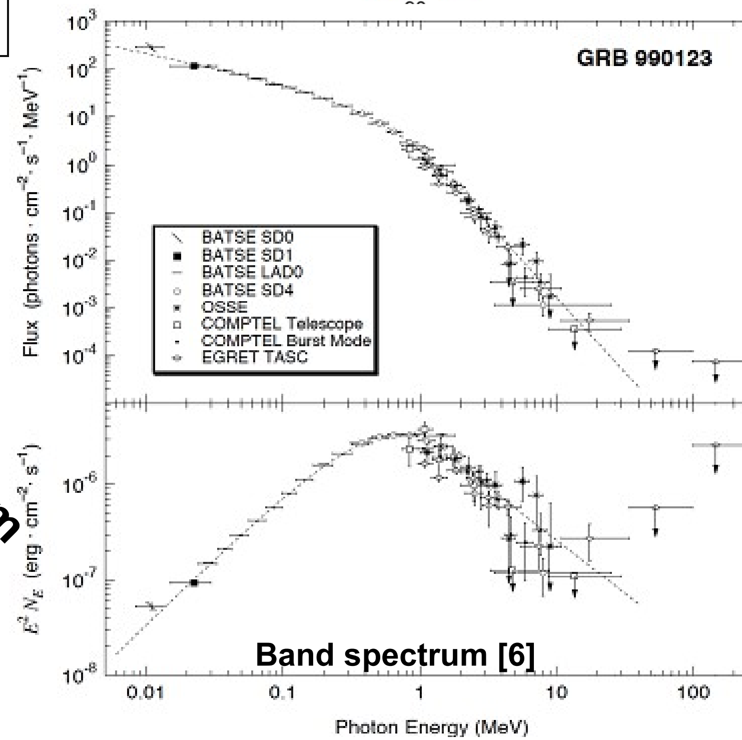

Band spectrum [6]

$$N(E) = K \begin{cases} \left(\dfrac{E}{100\mathrm{keV}}\right)^{\alpha} \exp\left[\dfrac{(2+\alpha)E}{E_p}\right] & , \ E \leq \left(\dfrac{\alpha-\beta}{2+\alpha}\right) E_p \\ \left(\dfrac{E}{100\mathrm{keV}}\right)^{\beta} \exp\left(\beta-\alpha\right) \left[\dfrac{(\alpha-\beta)E_p}{(2+\alpha)100\mathrm{keV}}\right] & , \ E > \left(\dfrac{\alpha-\beta}{2+\alpha}\right) E_p \end{cases}$$

[5] Meegan, C. A., Fishman, G. J., Wilson, R. B., et al. 1992, Nature, 355, 143
[6] Band, D. L. 2003, ApJ, 588, 945

First GRBs classification

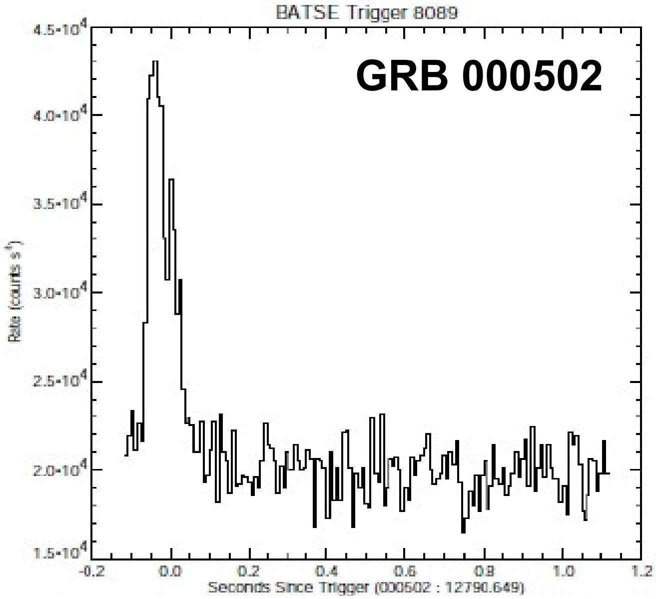

BATSE T_{90} distribution [7–10]

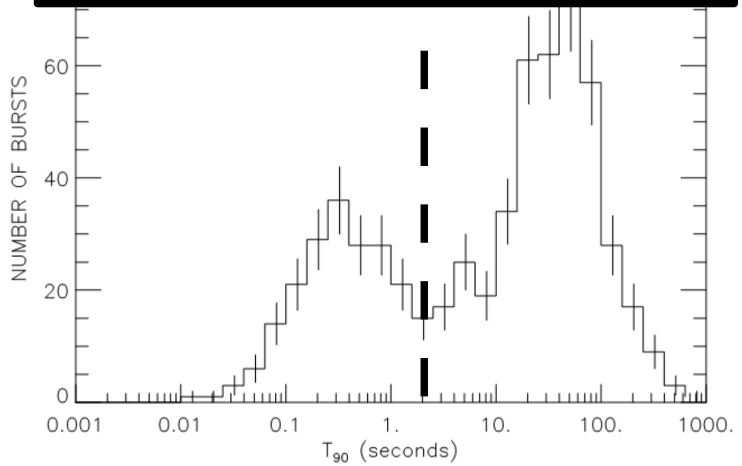

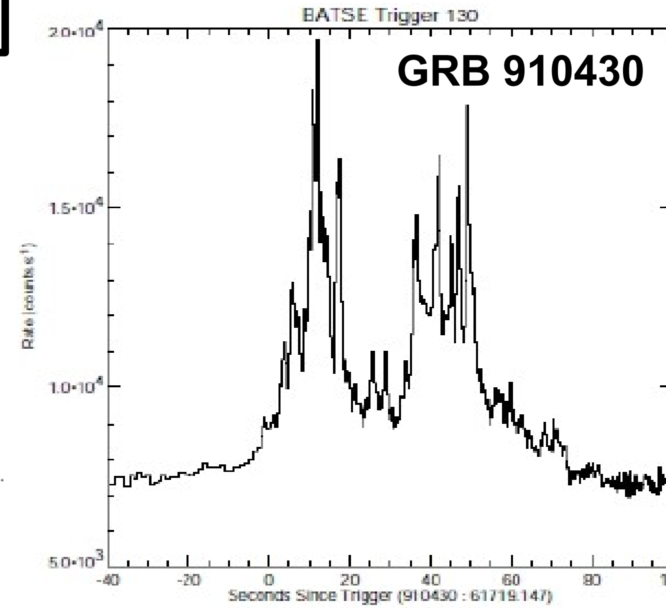

T_{90}<2 s $\Rightarrow$ Short GRBs

Spectra: sistematically harder.
Progenitor: *NS mergers* [11–14].
Origin: cosmological.
Physics: nuclear matter, $\nu\bar{\nu}\to e^+e^-$, accretion, r-process, GW.

T_{90}>2 s $\Rightarrow$ Long GRBs

Spectra: sistematically softer.
Progenitor: *collapsar* [15].
Origin: cosmological.
Physics: direct collapse to a BH, accretion disks.

[7] Klebesadel, R.W. 1992, in GRBs –Observations,Analyses&Theories, ed. C. Ho, R.I. Epstein, & E.E. Fenimore (Cambridge University Press), 161-168
[8] Dezalay, J.-P., Barat, C., Talon, R., et al. 1992, in American Institute of Physics Conference Series, Vol. 265, American Institute of Physics Conference Series, ed. W. S. Paciesas &G. J. Fishman, 304-309
[9] Kouveliotou, C., Meegan, C. A., Fishman, G. J., et al. 1993, ApJ, 413, L101
[10] Tavani, M. 1998, ApJ, 497, L21
[11] Goodman, J. 1986, ApJL, 308, L47
[12] Paczynski, B. 1986, 1pJL, 308, L43
[13] Eichler, D., Livio, M., Piran, T., & Schramm, D.N. 1989, Nature, 340, 126
[14] Narayan, R., Piran, T., & Shemi, A. 1991, ApJL, 379, L17
[15] Woosley, S. E. 1993, ApJ, 405, 273

Beppo-SAX and the afterglow discovery

Narrow field Instruments (NFI):
- Low Energy Concentrator Spectrometer (LECS) 0.1-10 keV.
- Medium Energy CS (MECS) 1.3-10 keV.
- High Pressure Gas Scintillator Proportional Counter (HPGSPC) 4-120 keV
- Phoswich Detection System (PDS) 15-300 keV.

Wide Field Camera (2 units) 2-30 keV.

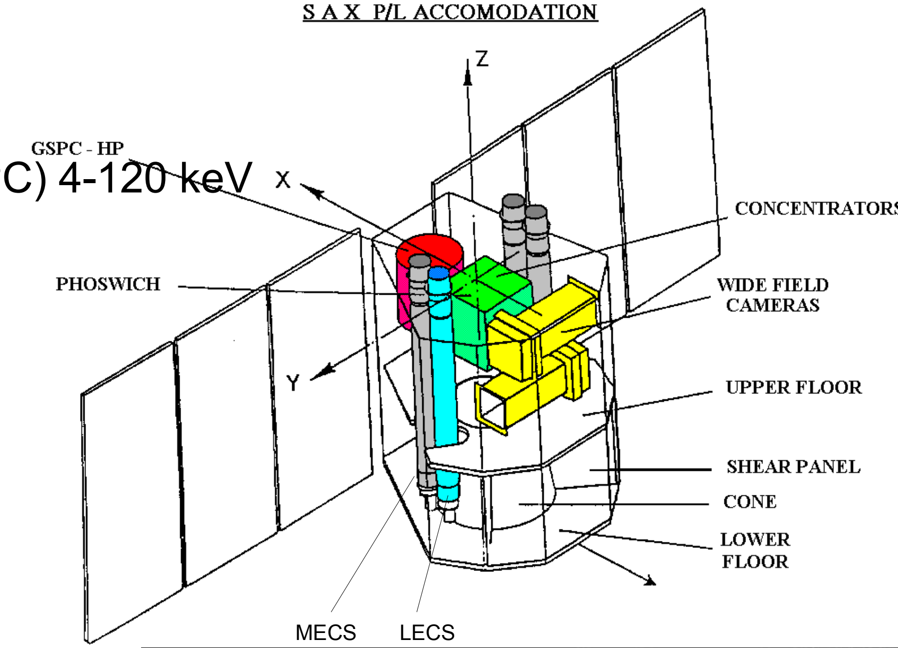

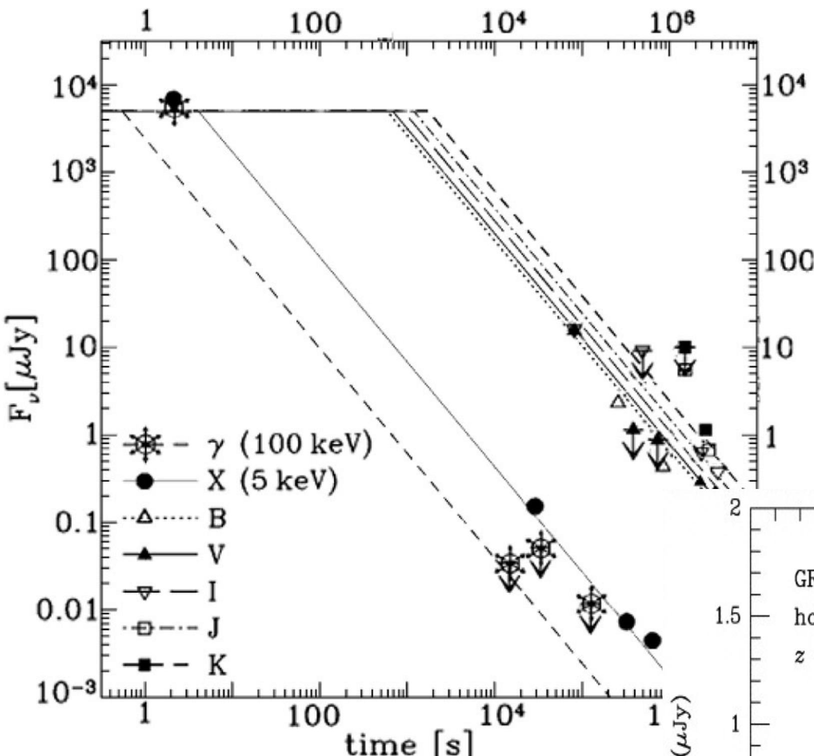

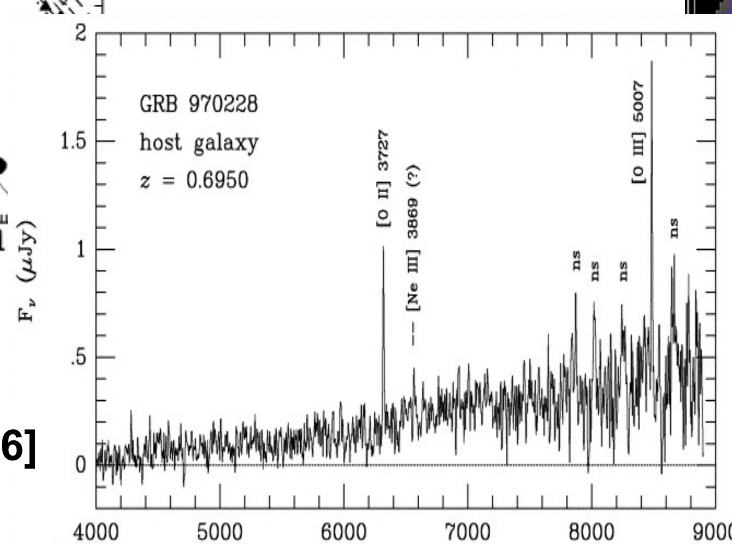

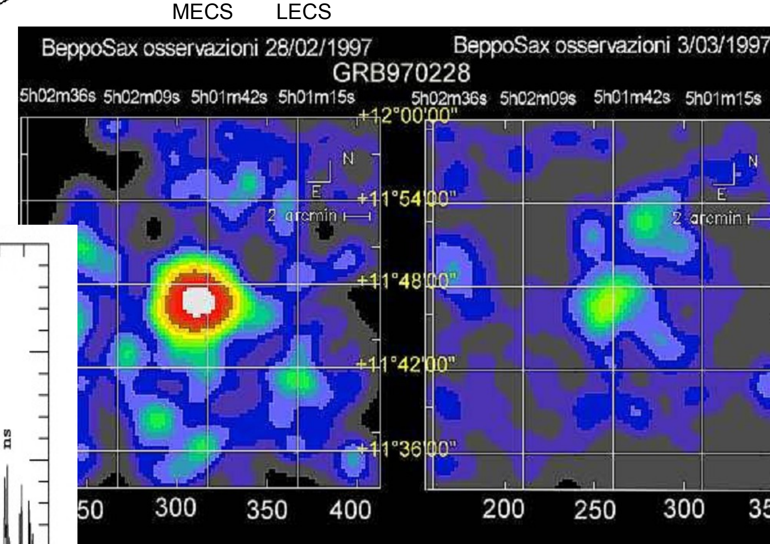

Cosmological origin of GRBs [16]

[16] van Paradijs, J., Groot, P. J., Galama, T., et al. 1997, Nature, 386, 686

The dawn of the GRB-SN connection [17]

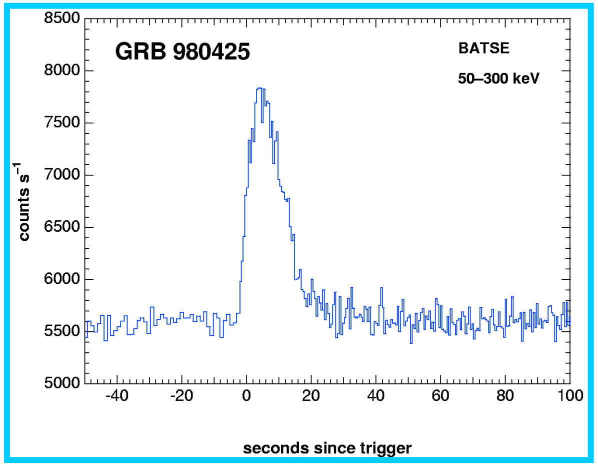

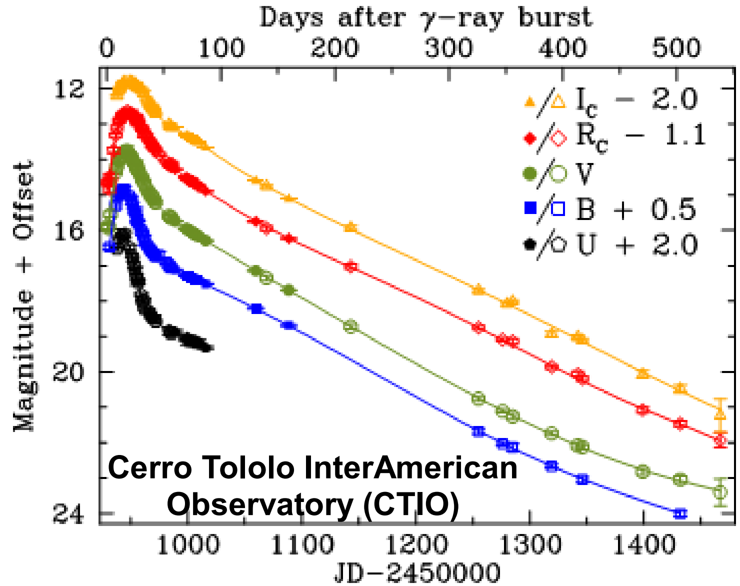

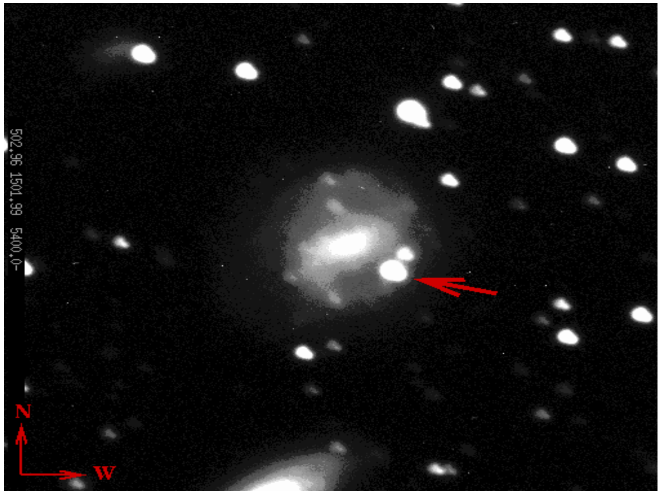

GRB-SN Ib/c connections imply:

- **association with massive stars;**
- **star-forming regions.**
- **no H and no/ weak He lines;**
- **birth in binary systems [18].**

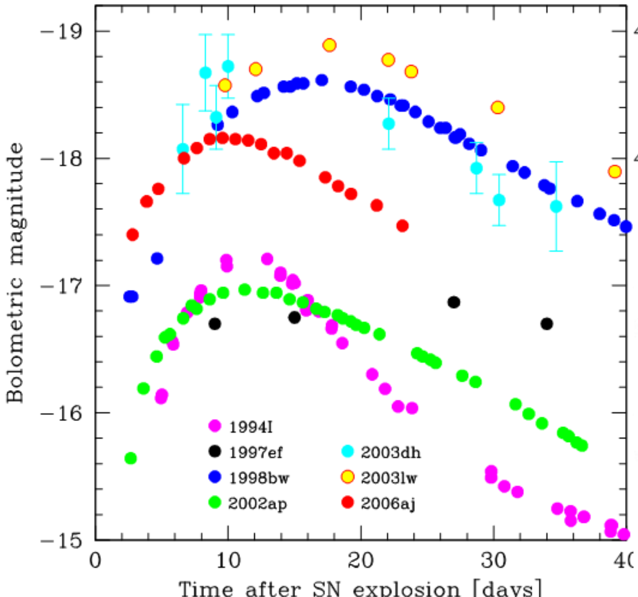

Additional properties:

- **Broad line spectra → high expansion velocity (0.1 c);**
- **larger observed magnitudes;**

Further energy injection

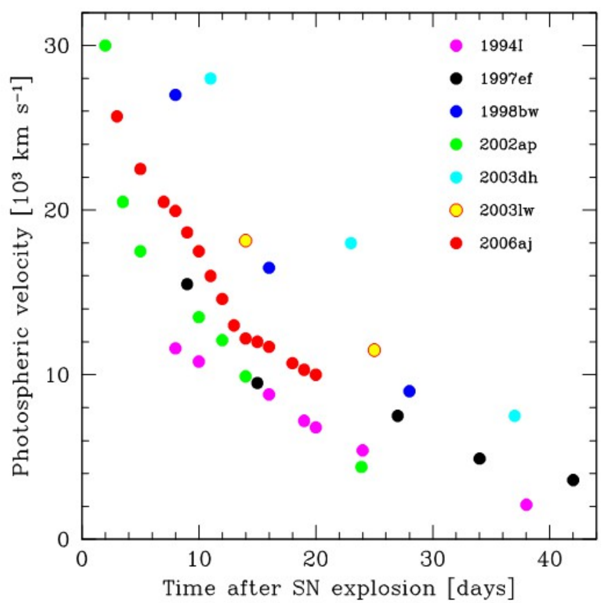

[17] Galama, T. J., Vreeswijk, P. M., van Paradijs, J., et al. 1998, Nature, 395, 670
[18] Nomoto, K., Yamaoka, H., Pols, O. R., et al. 1994, Nature, 371, 227

The Induced Gravitational Collapse (IGC)

A binary progenitor system [19]

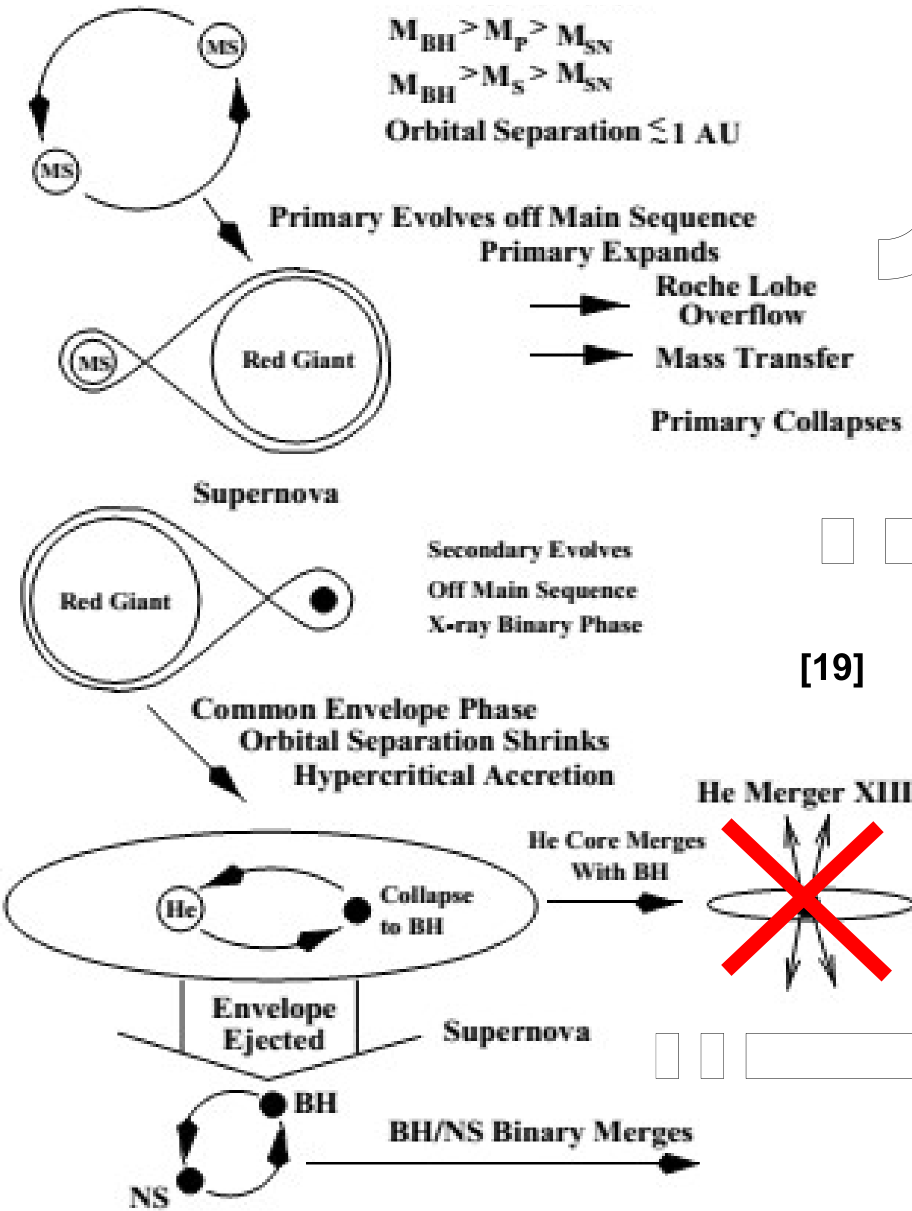

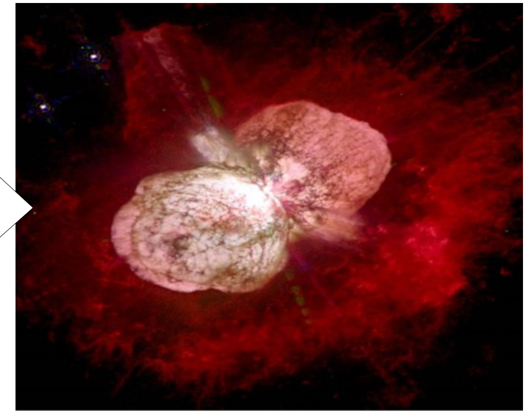

Massive Binary
(Eta Carinae, Porb=5.5 yr)

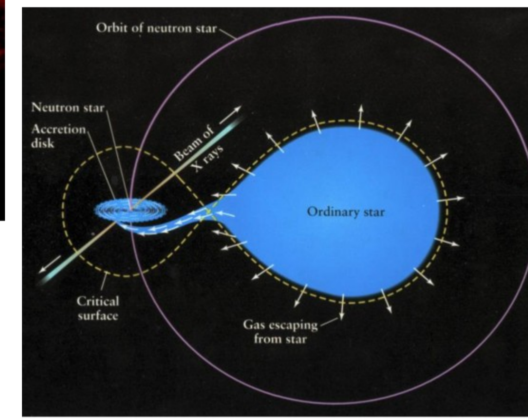

Massive Star-Neutron Star X Ray Binary
(Centaurus X-3, Porb=2.1 days)

The IGC progenitor system [20,21]

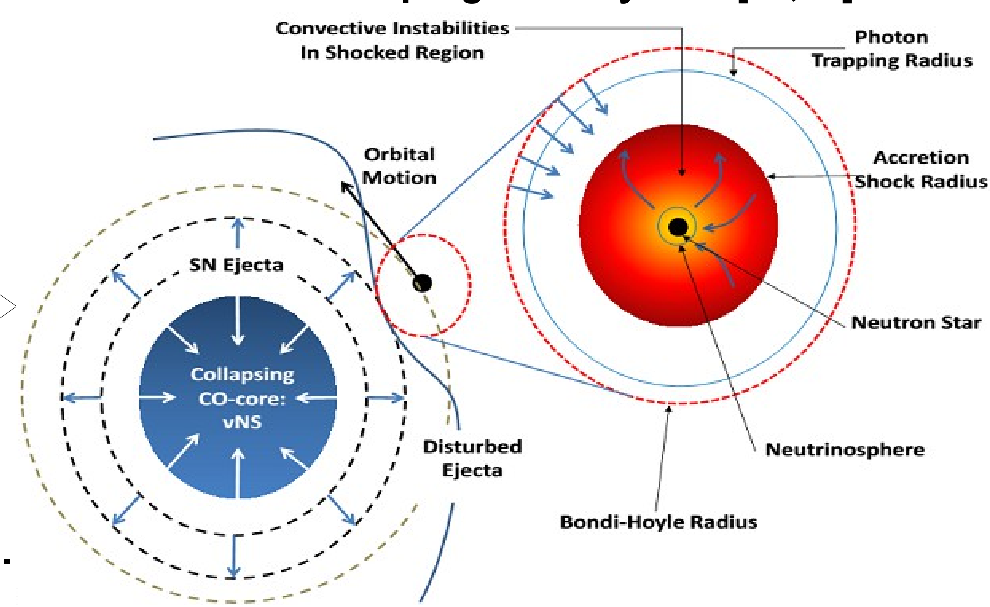

[19] C.L.Fryer, S.E. Woosley and D.H. Hartmann, ApJ, 526, 152 (1999).
[20] J.A. Rueda & R. Ruffini, ApJL, 758, L7 (2012).
[21] L. Izzo, J.A. Rueda and R. Ruffini, A&A, 548, L5 (2012)

The fireshell model for GRBs [22–24]

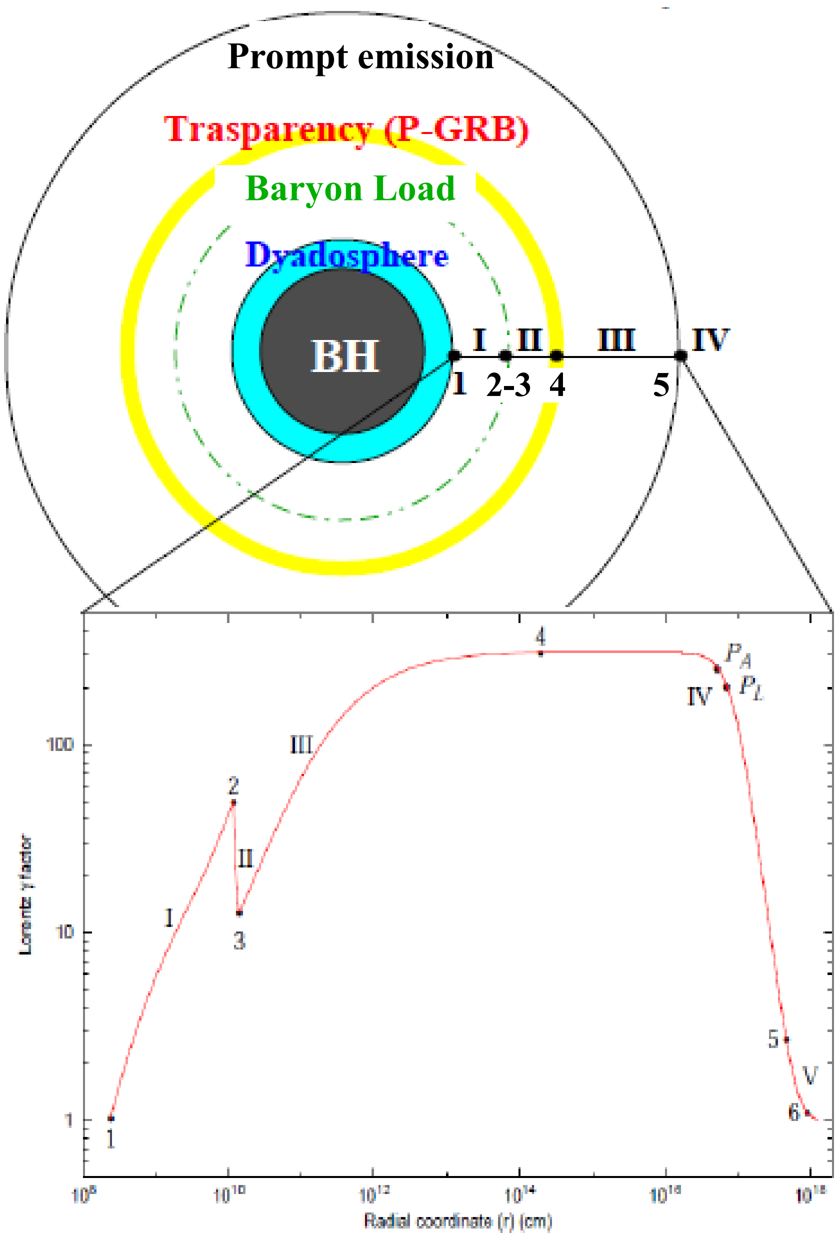

– An optically thick $e^{\pm}$ plasma with energy $\boxed{E^{tot}_{\pm}}$ is formed in the gravitational collapse to a black hole.

– The expanding $e^{\pm}$ *fireshell* engulfs the baryons left over in the collapse to BH, described by the baryon load $\boxed{B=M_B c^2/E^{tot}_{\pm}}$, and thermalizes with the baryons.

– The fireshell self-accelerates to ultra-relativistic velocities up to the transparency and the Proper-GRB (P-GRB) is emitted.

– After transparency, the optically thin shell of baryons slows down by collisions with the Circum Burst Medium (CBM) with density $\boxed{n_{CBM}}$, giving rise to the prompt emission. The CBM is modeled by the filling factor, which takes into account filamentary structures of the medium, $\boxed{R=A_{eff}/A_{vis}}$.

– This formalism can be applied to any optically thick $e^{\pm}$–plasma, like the one created via $\nu\bar{\nu}\rightarrow e^{+}e^{-}$ [14] in NS mergers, or in the accretion onto BHs [15].

[22] Ruffini, R., Bianco, C. L., Fraschetti, F., Xue, S., & Chardonnet, P. 2001, ApJ, 555, L117
[23] Ruffini, R., Bianco, C. L., Fraschetti, F., Xue, S., & Chardonnet, P. 2001, ApJ, 555, L113
[24] Ruffini, R., Bianco, C. L., Fraschetti, F., Xue, S., & Chardonnet, P. 2001, ApJ, 555, L107

The fireshell model for GRBs [22–24]

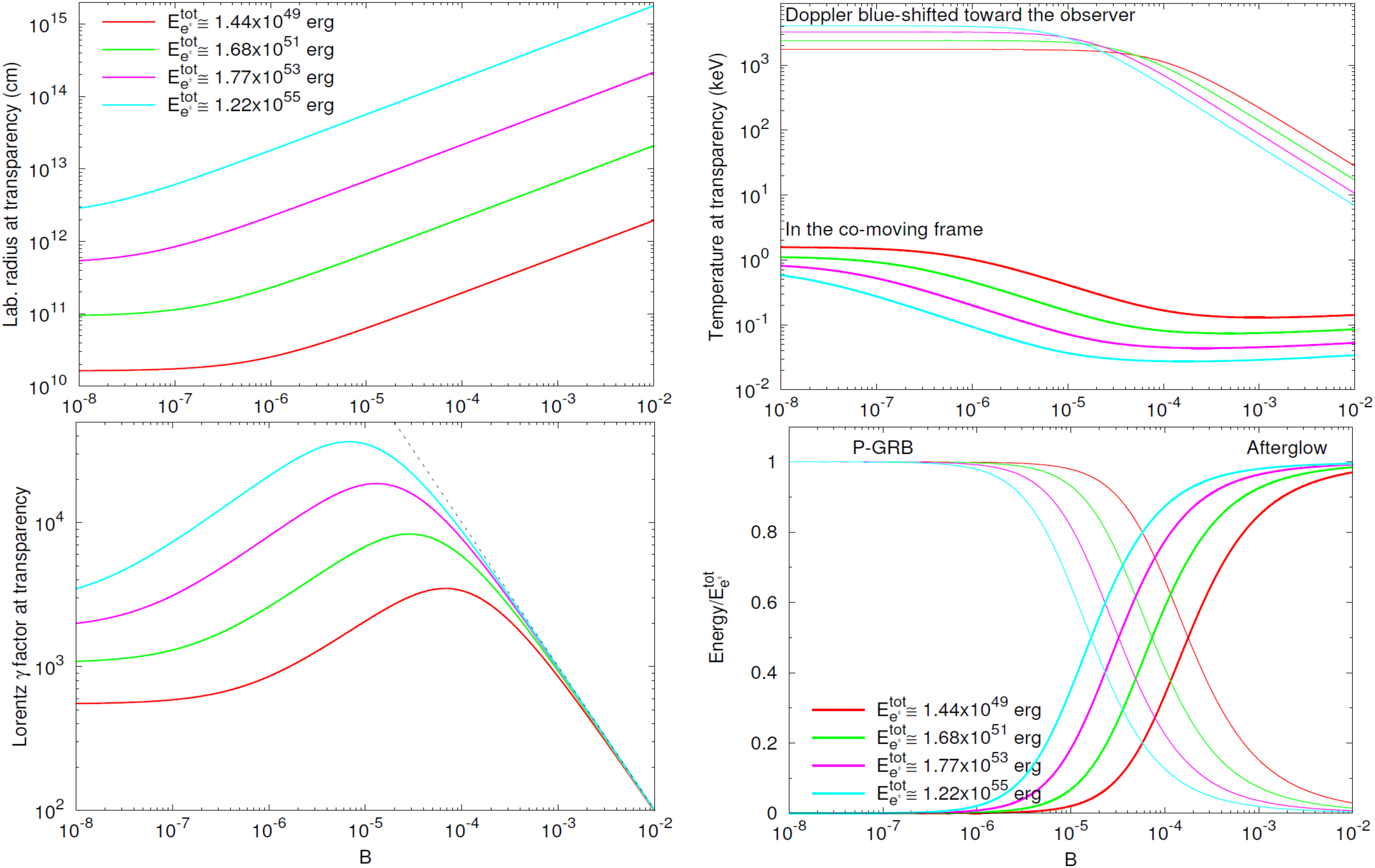

[22] Ruffini, R., Bianco, C. L., Fraschetti, F., Xue, S., & Chardonnet, P. 2001, ApJ, 555, L117
[23] Ruffini, R., Bianco, C. L., Fraschetti, F., Xue, S., & Chardonnet, P. 2001, ApJ, 555, L113
[24] Ruffini, R., Bianco, C. L., Fraschetti, F., Xue, S., & Chardonnet, P. 2001, ApJ, 555, L107

The *Swift* revolution (2004 – ...)

Burst Alert Telescope (BAT) 15–150 keV
- GRB trigger and location (1–4 arc-minutes);

X-ray Telescope (XRT) 0.3–10 keV
- ~2 arcseconds error circle radius location;

Ultraviolet/Optical Telescope (UVOT)
- sub-arcsecond position;
- optical and UV photometry at 170–650 nm.

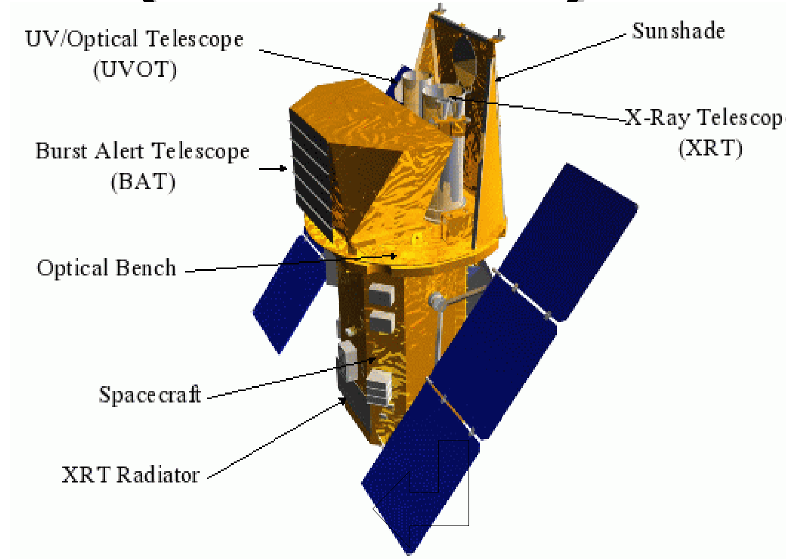

Short GRBs with extended emission [25] or disguised short γ-ray flashes (DS-GRFs)
Spike-like emission + a softer extended tail [26].

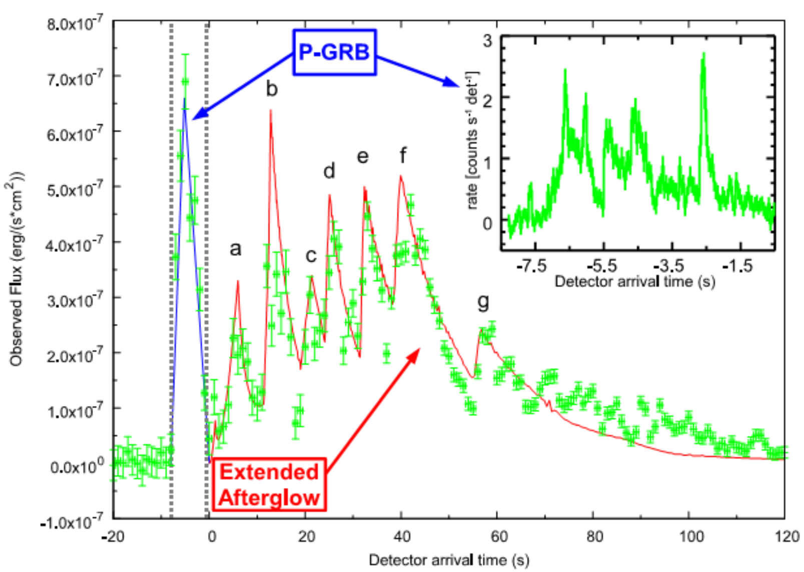

X-ray afterglow

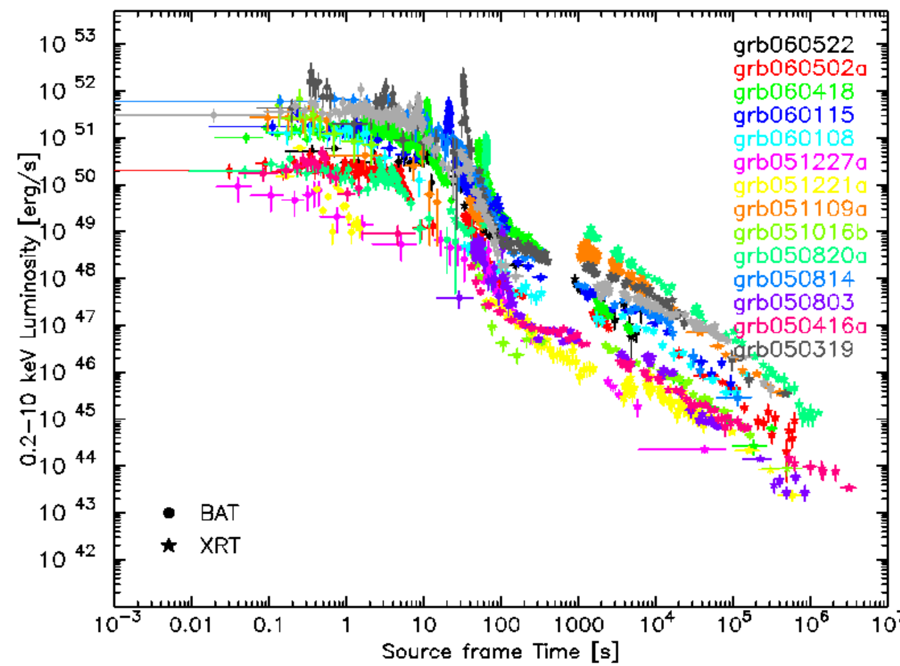

[25] Norris, J. P., & Bonnell, J. T. 2006, ApJ, 643, 266
[26] Caito, L., Amati, L., Bernardini, M. G., et al. 2010, A&A, 521, A80+

The *Swift* revolution (2004 – ...)

Burst Alert Telescope (BAT) 15–150 keV
- GRB trigger and location (1–4 arc-minutes);

X-ray Telescope (XRT) 0.3–10 keV
- ~2 arcseconds error circle radius location;

Ultraviolet/Optical Telescope (UVOT)
- sub-arcsecond position;
- optical and UV photometry at 170–650 nm.

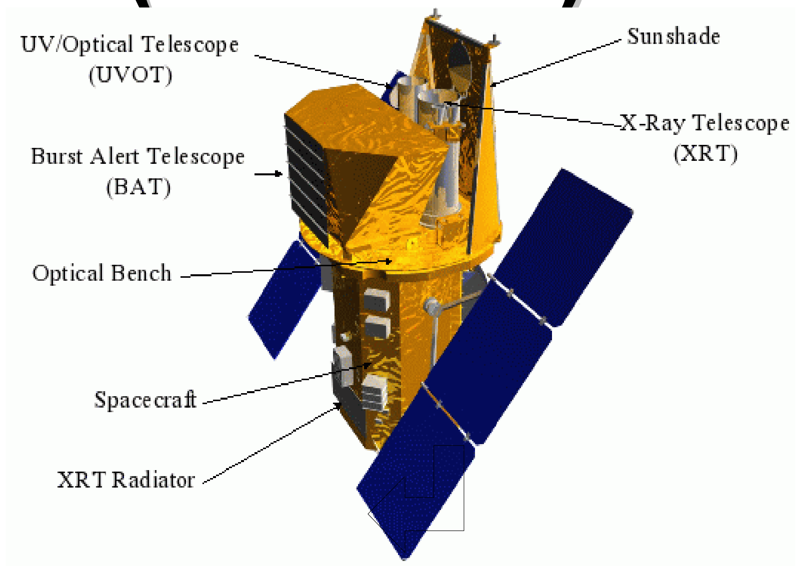

Short GRBs with extended emission [25] or disguised short γ-ray flashes (DS-GRFs)

No associated SN[27] → NS-WD mergers [26].

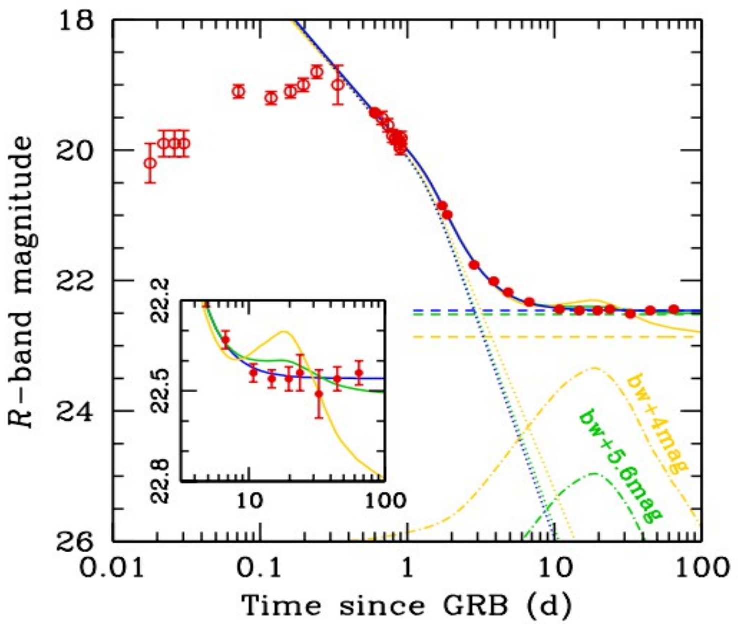

X-ray afterglow

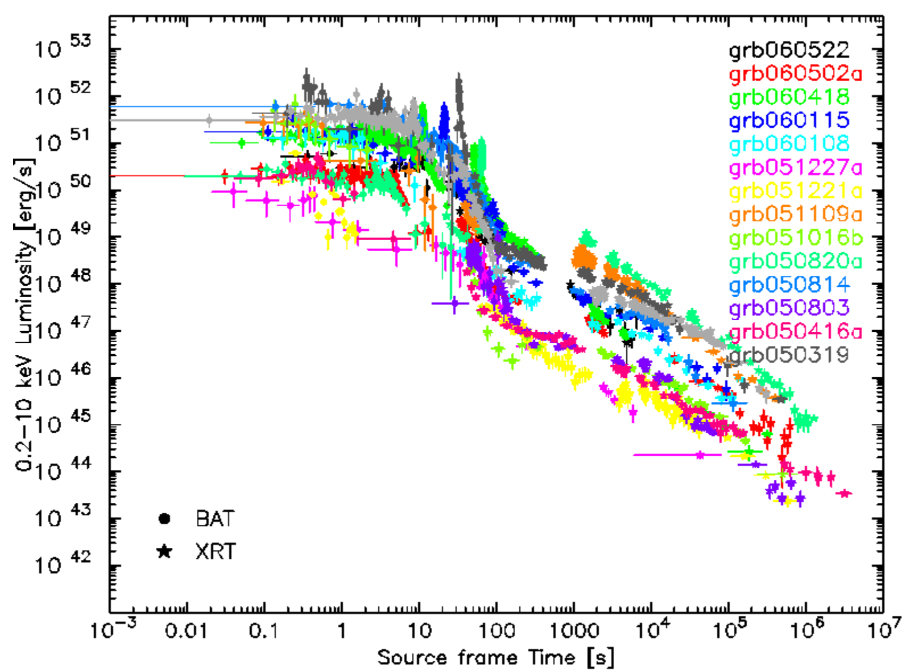

[27] Della Valle, M., Chincarini, G., Panagia, N., et al. 2006, Nature, 444, 1050

The Fermi era (2008 – ...)

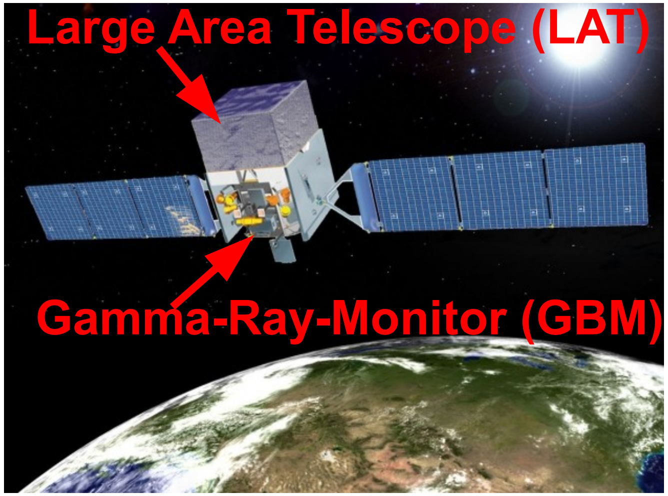

http://fermi.gsfc.nasa.gov/

Thermal component: GRB 110721A

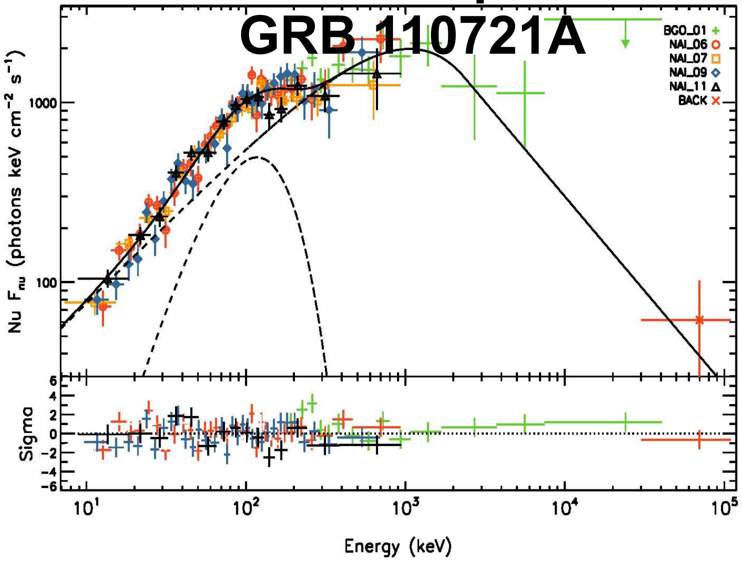

GeV emission: GRB 080916C

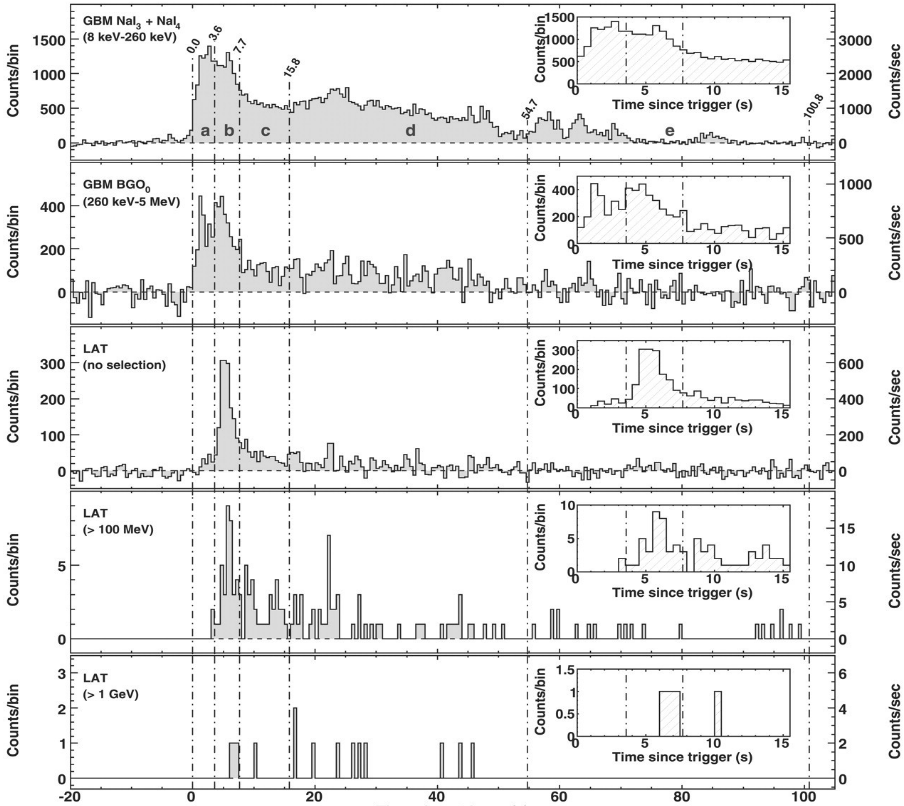

GeV emission in short and long bursts

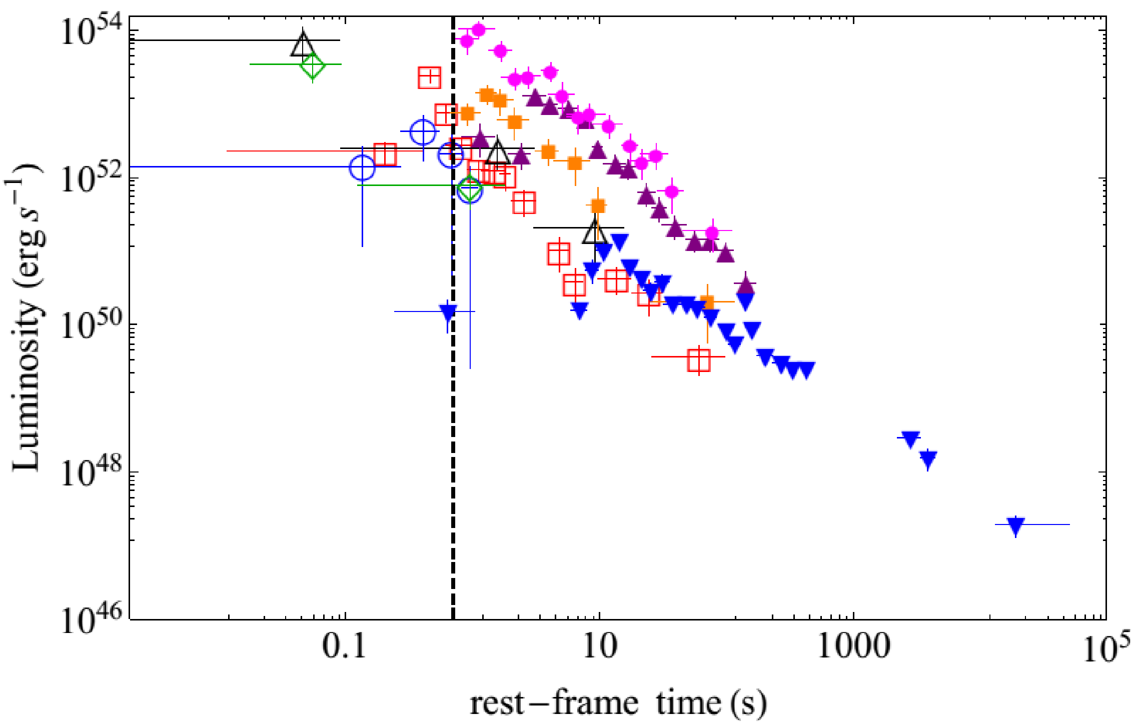

A further classification of GRBs?
A forensic investigations

$E_{p,i}$-E_{iso} relations for short and long GRBs

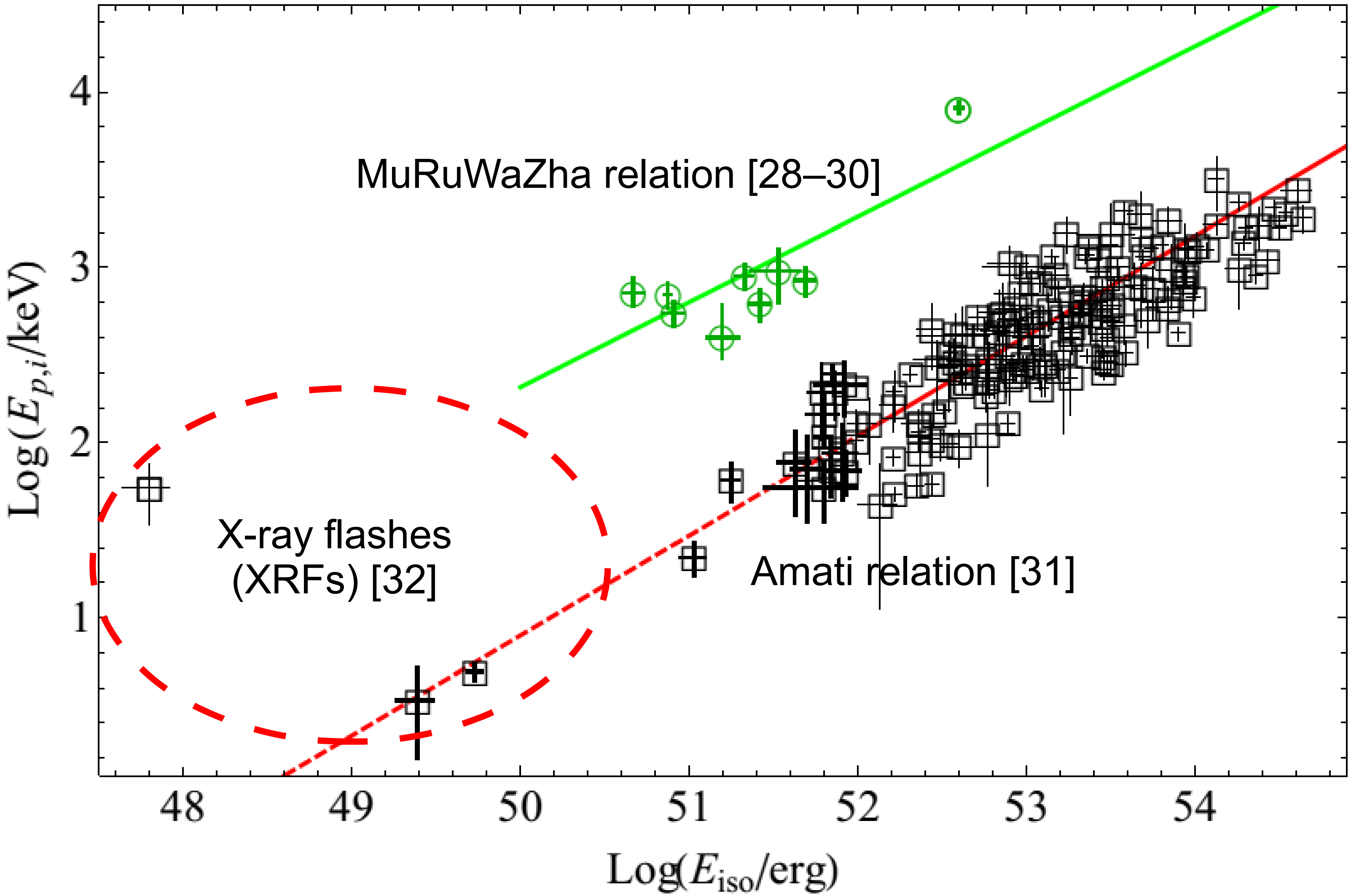

This is as much one can extract from γ-rays? What about other energy bands?

[28] Zhang, F.-W., Shao, L., Yan, J.-Z., & Wei, D.-M. 2012, ApJ, 750, 88.

[29] Calderone, G., Ghirlanda, G., Ghisellini, G., et al. 2015, MNRAS, 448, 403.

[30] Ruffini, R., Muccino, M., Kovacevic, M., et al. 2015, ApJ, 808, 190

[31] Amati, L., & Della Valle, M. 2013, International Journal of Modern Physics

[32] Soderberg, A. M., Kulkarni, S. R., Nakar, E., et al. 2006, Nature, 442, 1014

$E_{p,i}$-E_{iso} relations for short and long GRBs [28–32]

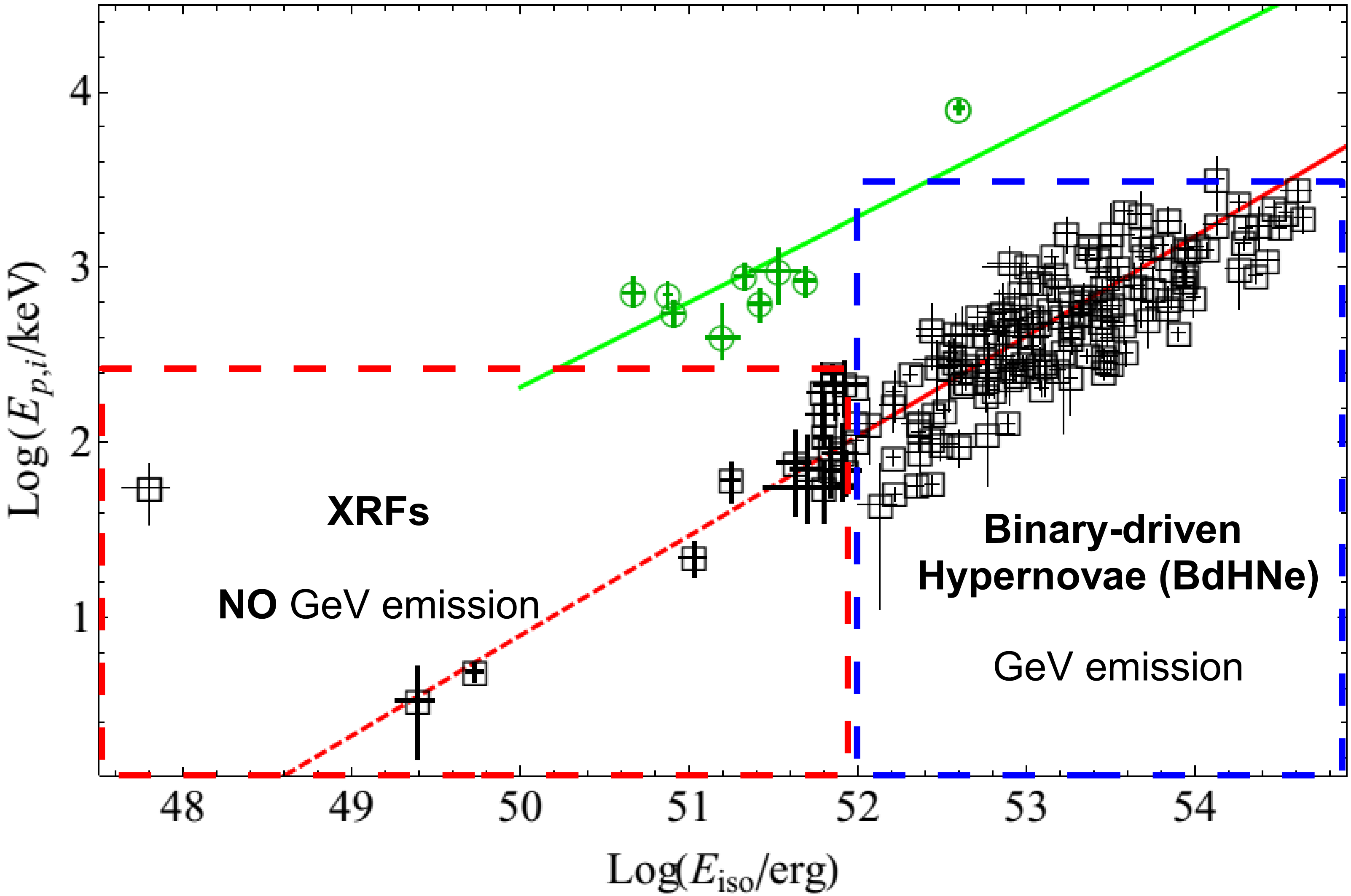

[28] Zhang, F.-W., Shao, L., Yan, J.-Z., & Wei, D.-M. 2012, ApJ, 750, 88.

[29] Calderone, G., Ghirlanda, G., Ghisellini, G., et al. 2015, MNRAS, 448, 403.

[30] Ruffini, R., Muccino, M., Kovacevic, M., et al. 2015, ApJ, 808, 190

[31] Amati, L., & Della Valle, M. 2013, International Journal of Modern Physics

[32] Soderberg, A. M., Kulkarni, S. R., Nakar, E., et al. 2006, Nature, 442, 1014

The X-ray flashes (XRFs) [33]

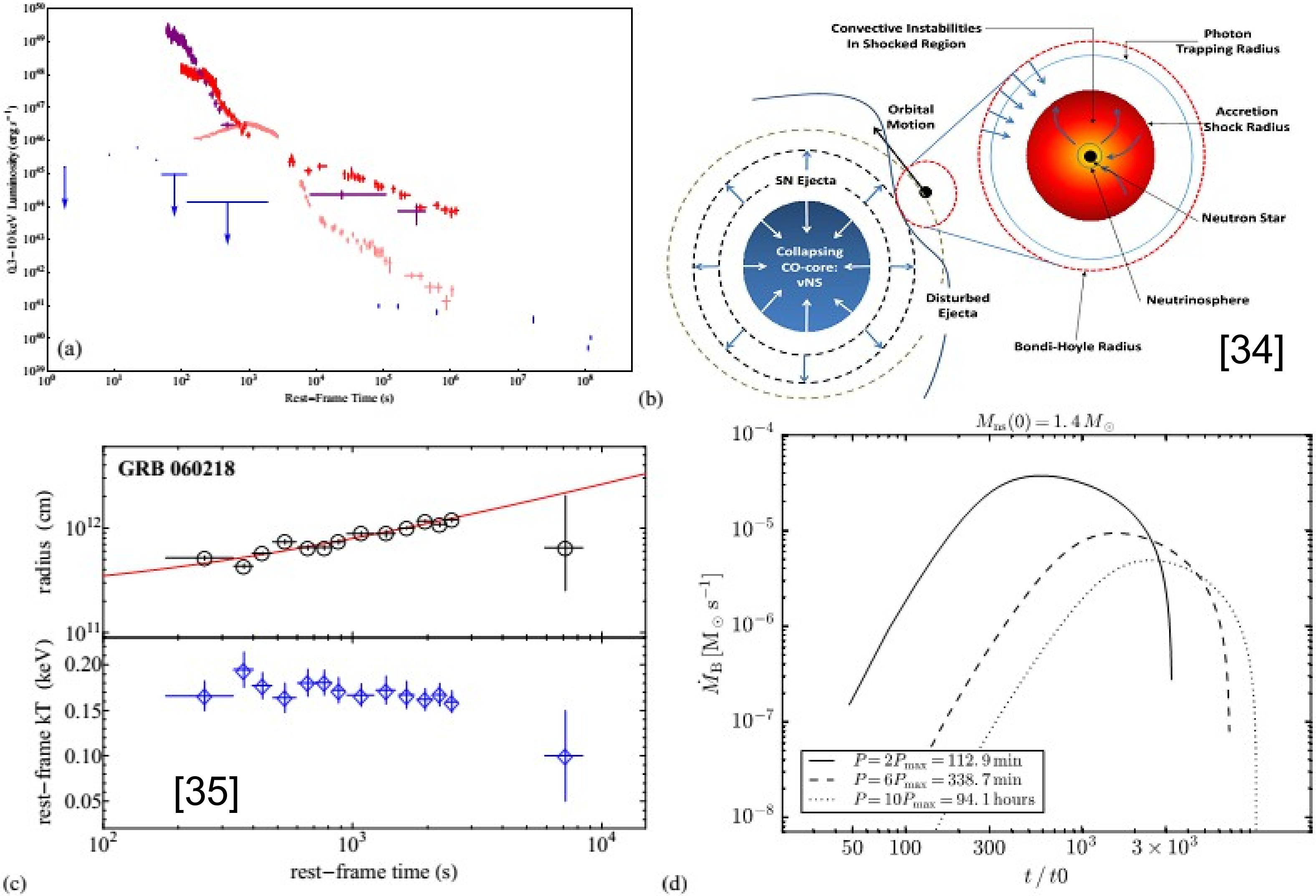

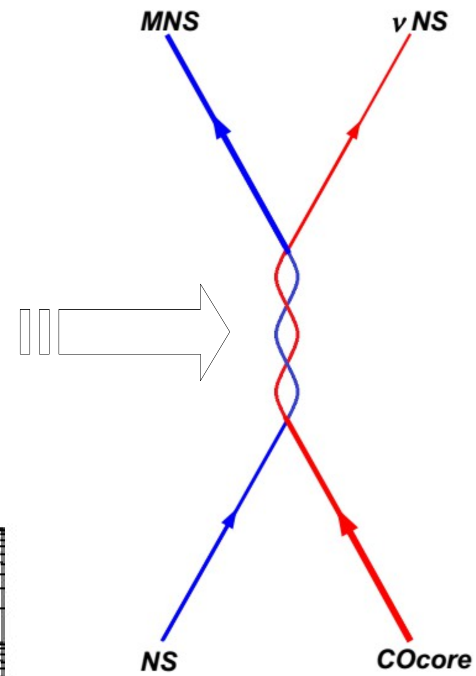

- No BH formation;
- No GeV emission;
- Associated SN Ib/c;
- $E_{iso} < 10^{52}$ erg explained by the accretion of the SN ejecta onto the companion NS.

[33] Ruffini, R., Rueda, J.A., Muccino, M., et al. 2016, arXiv:1602.02732
[34] Fryer, C. L., Rueda, J. A., & Ruffini, R. 2014, ApJ, 793, L36
[35] Campana, S., Mangano, V., Blustin, A. J., et al. 2006, Nature, 442, 1008

The binary-driven Hypernovae (BdHNe) [33]

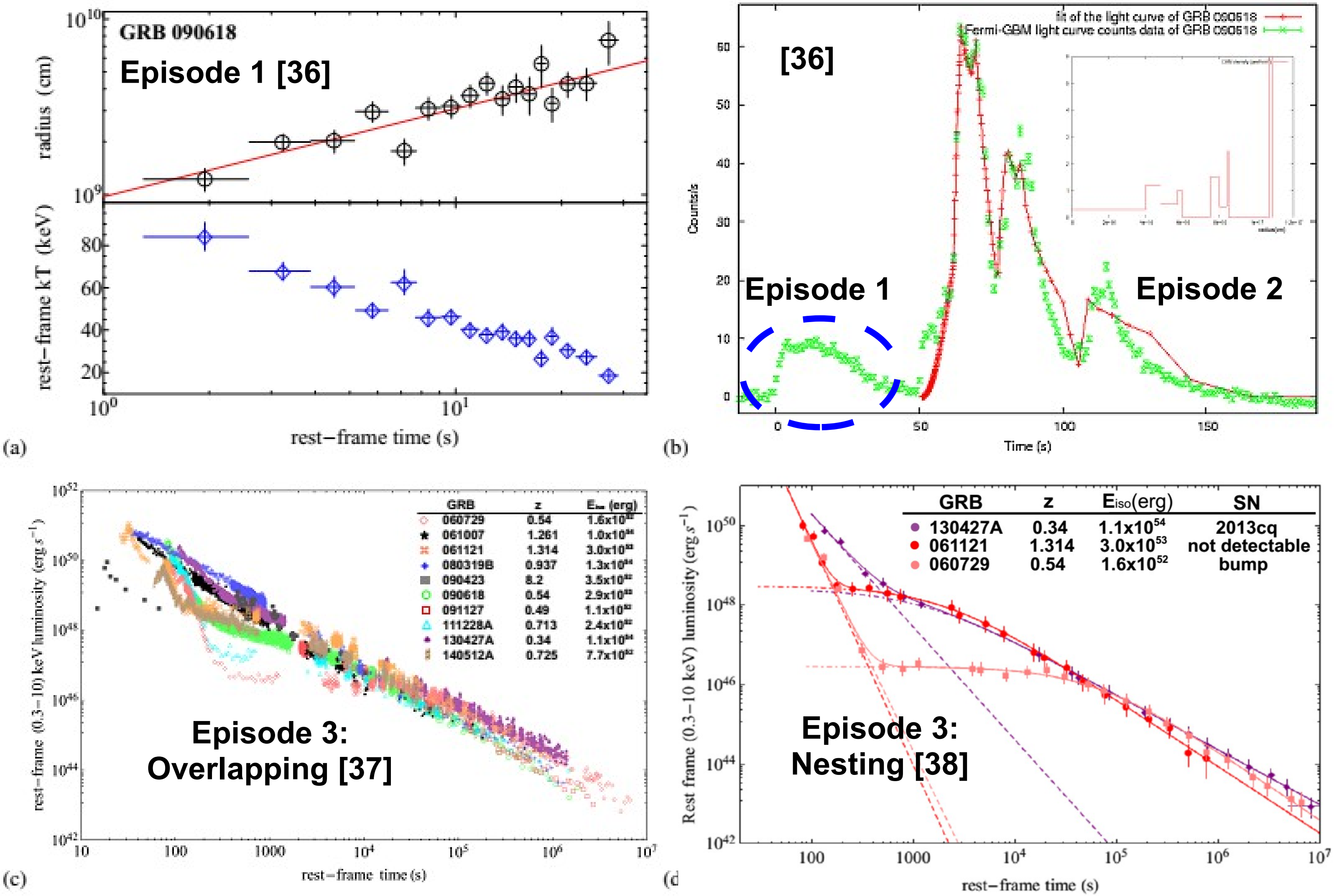

[36] Izzo, L., Ruffini, R., Penacchioni, A. V., et al. 2012, A&A, 543, A10
[37] Pisani, G. B., Izzo, L., Ruffini, R., et al. 2013, A&A, 552, L5
[38] Ruffini, R., Muccino, M., Bianco, C. L., et al. 2014, A&A, 565, L10

The binary-driven Hypernovae (BdHNe) [33]

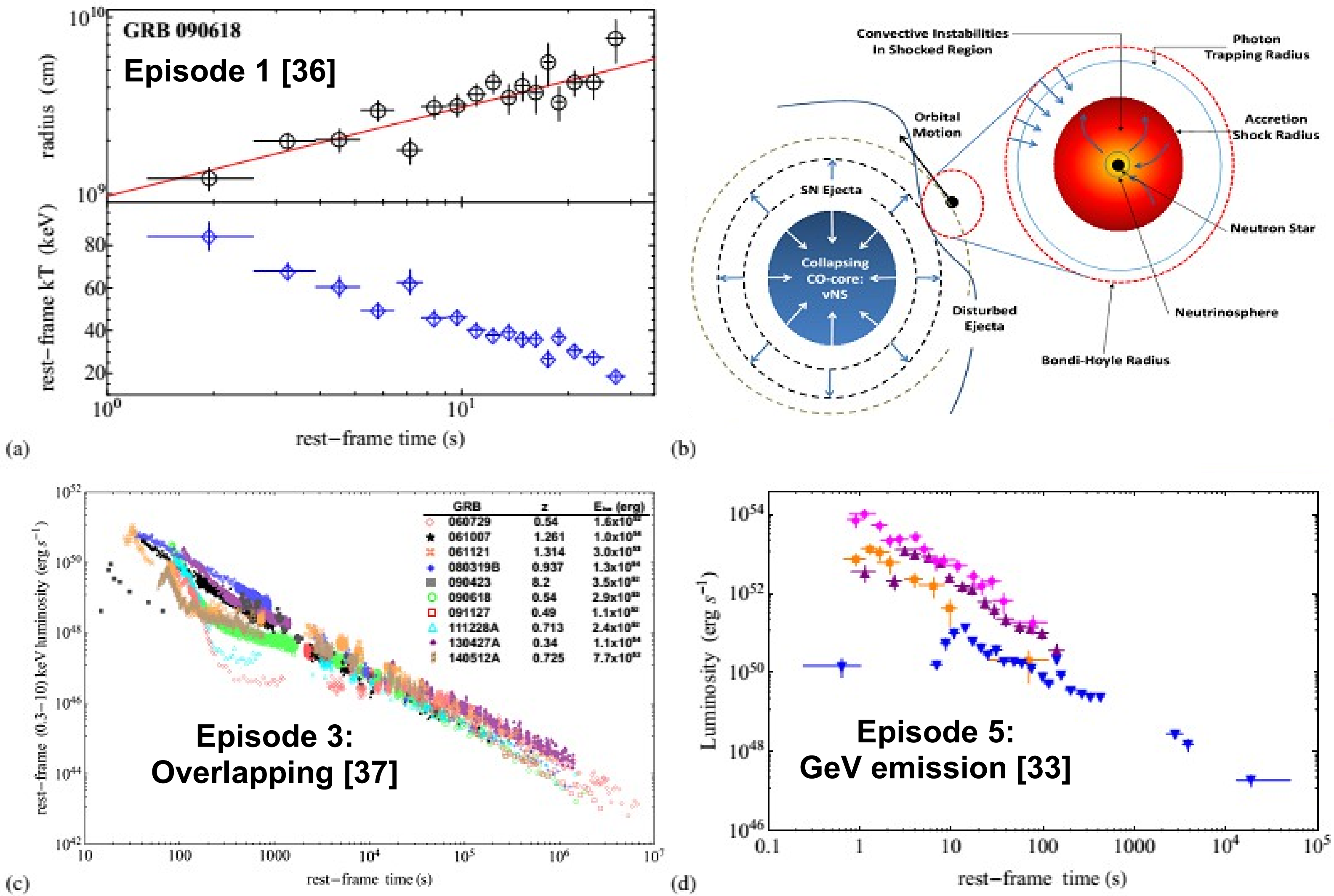

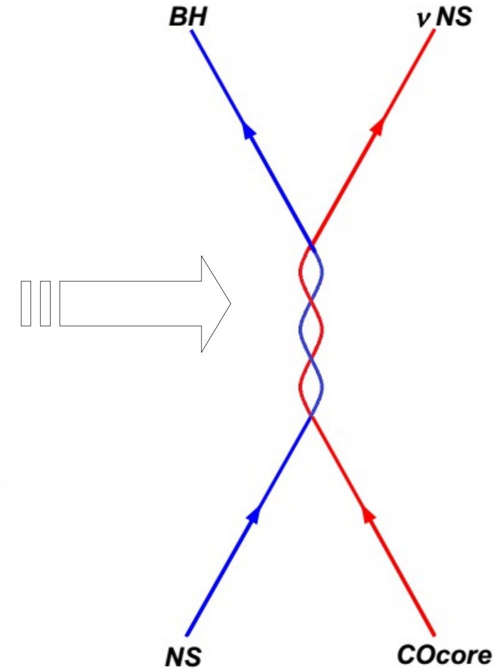

- BH formation;
- GeV emission;
- Associated SN Ib/c;
- $E_{iso} > 10^{52}$ erg explained by the emission of a GRB.

[36] Izzo, L., Ruffini, R., Penacchioni, A. V., et al. 2012, A&A, 543, A10
[37] Pisani, G. B., Izzo, L., Ruffini, R., et al. 2013, A&A, 552, L5
[38] Ruffini, R., Muccino, M., Bianco, C. L., et al. 2014, A&A, 565, L10

The binary-driven Hypernovae (BdHNe) [33]

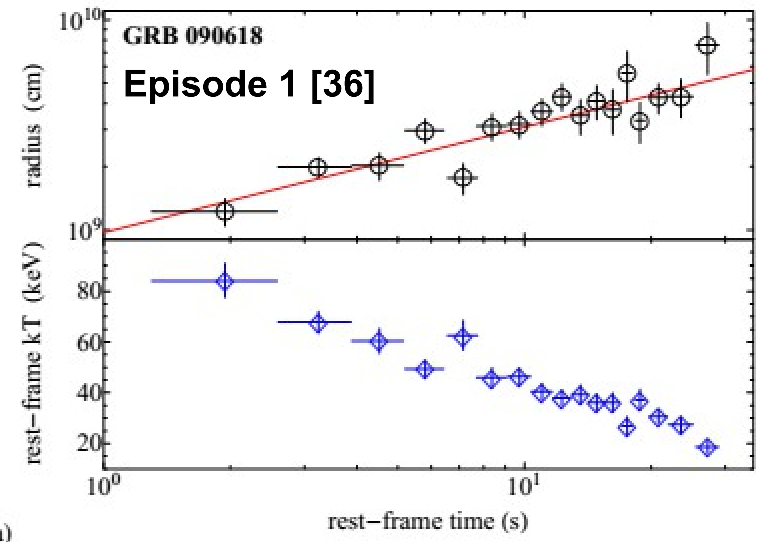

(a)

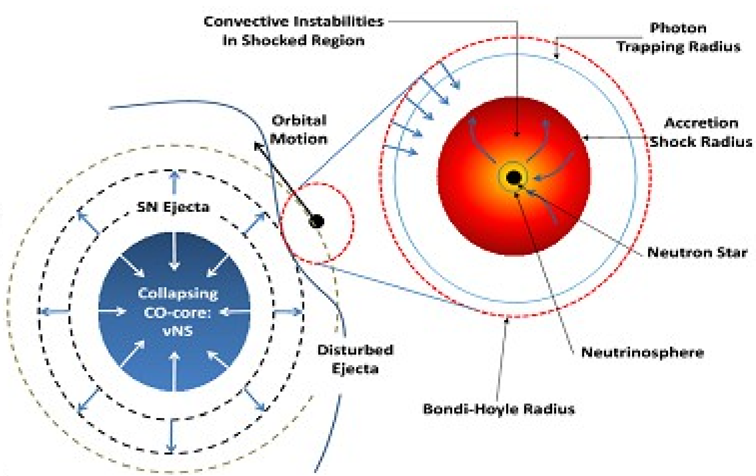

(b)

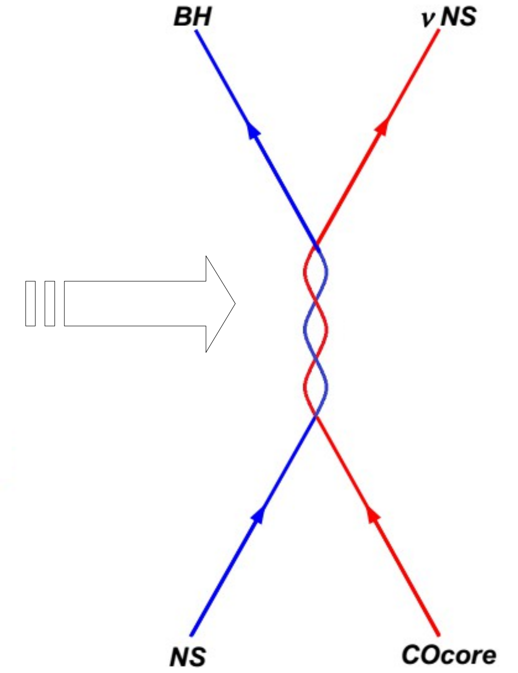

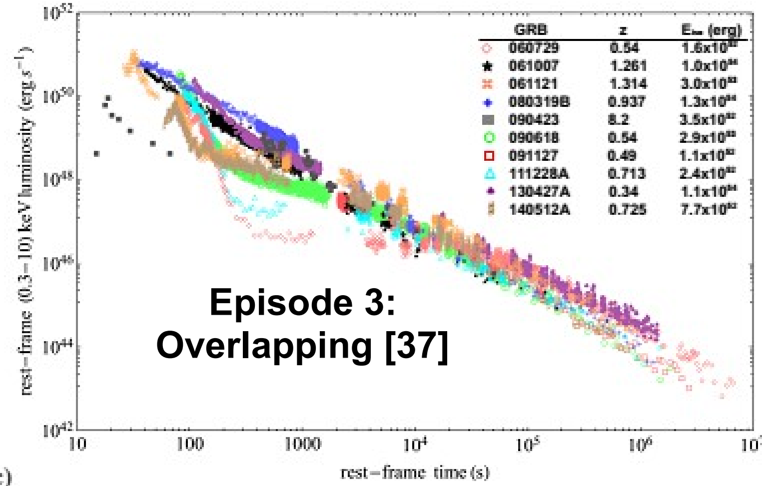

(c)

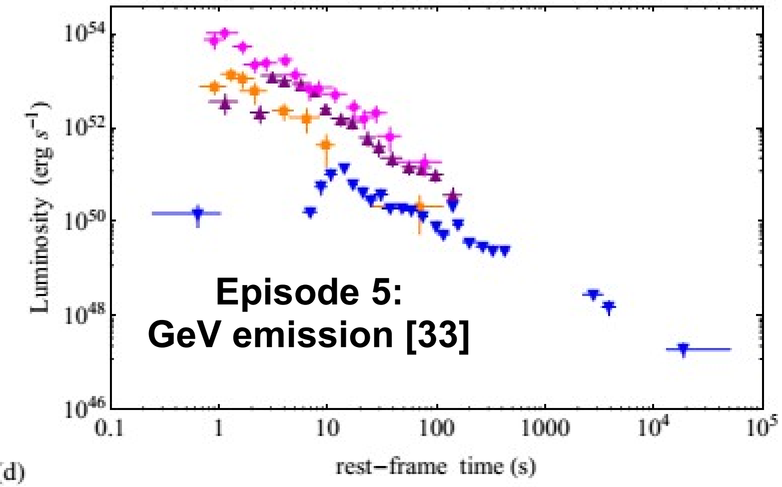

(d)

We proposed that the BH formation implies the presence of the GeV emission: it is the manifestation of the BH activity by accretion of residual matter [39].

[39] Ruffini, R., Wang, Y., Enderli, M., et al. 2015a, ApJ, 798, 10

$E_{p,i}$-E_{iso} relations for short and long GRBs (2)

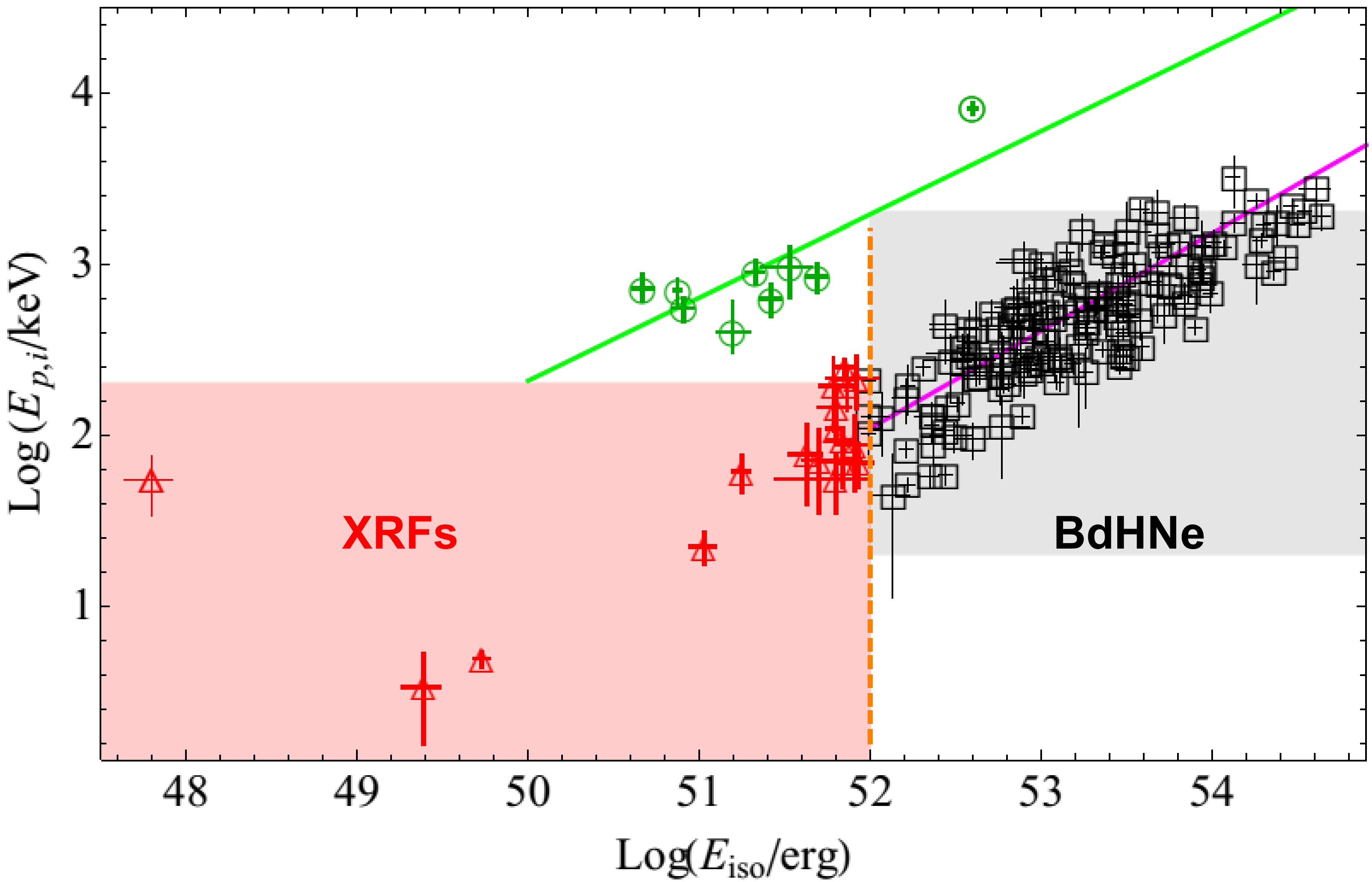

What about short bursts? Can we apply the same method used for long bursts?

[28] Zhang, F.-W., Shao, L., Yan, J.-Z., & Wei, D.-M. 2012, ApJ, 750, 88.

[29] Calderone, G., Ghirlanda, G., Ghisellini, G., et al. 2015, MNRAS, 448, 403.

[30] Ruffini, R., Muccino, M., Kovacevic, M., et al. 2015, ApJ, 808, 190

[31] Amati, L., & Della Valle, M. 2013, International Journal of Modern Physics

$E_{p,i}$-E_{iso} relations for short and long GRBs (2)

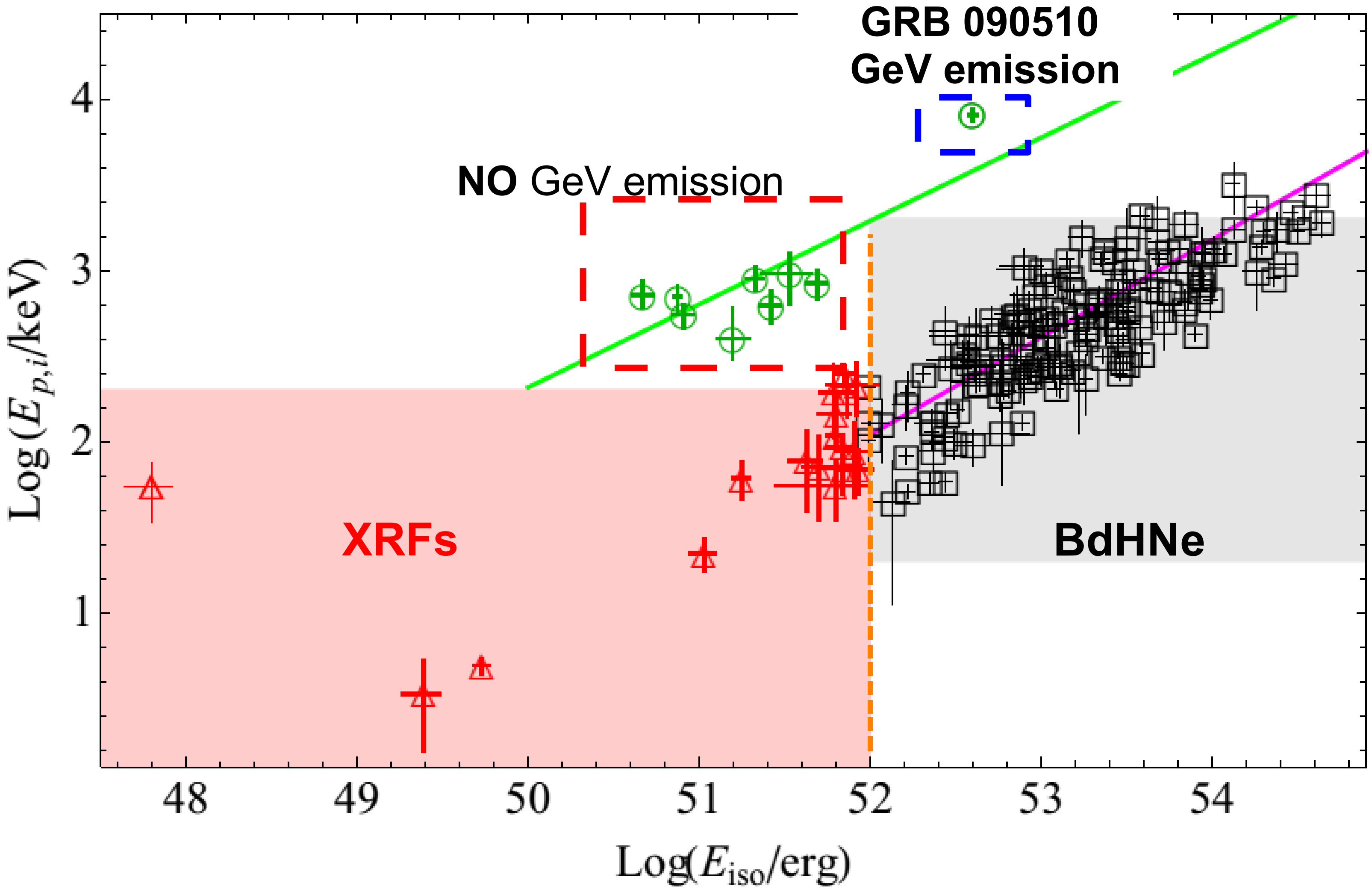

[28] Zhang, F.-W., Shao, L., Yan, J.-Z., & Wei, D.-M. 2012, ApJ, 750, 88.

[29] Calderone, G., Ghirlanda, G., Ghisellini, G., et al. 2015, MNRAS, 448, 403.

[30] Ruffini, R., Muccino, M., Kovacevic, M., et al. 2015, ApJ, 808, 190

[31] Amati, L., & Della Valle, M. 2013, International Journal of Modern Physics

$E_{p,i}$-E_{iso} relations for short and long GRBs (2)

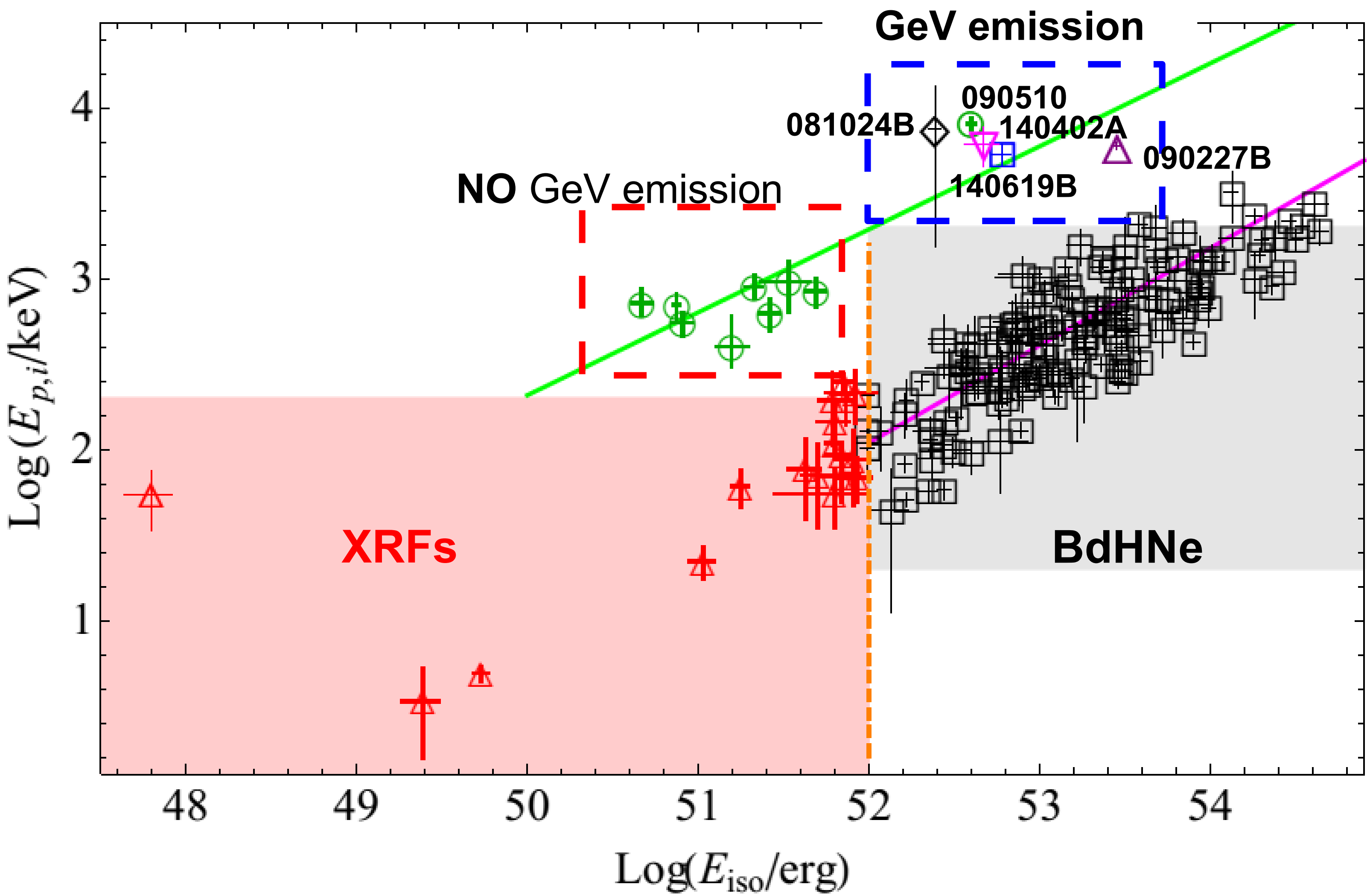

Again, what kind of information can we extract from other energy bands?

[28] Zhang, F.-W., Shao, L., Yan, J.-Z., & Wei, D.-M. 2012, ApJ, 750, 88.
[29] Calderone, G., Ghirlanda, G., Ghisellini, G., et al. 2015, MNRAS, 448, 403.
[30] Ruffini, R., Muccino, M., Kovacevic, M., et al. 2015, ApJ, 808, 190
[31] Amati, L., & Della Valle, M. 2013, International Journal of Modern Physics

The short gamma-ray flashes (S-GRFs) [33]

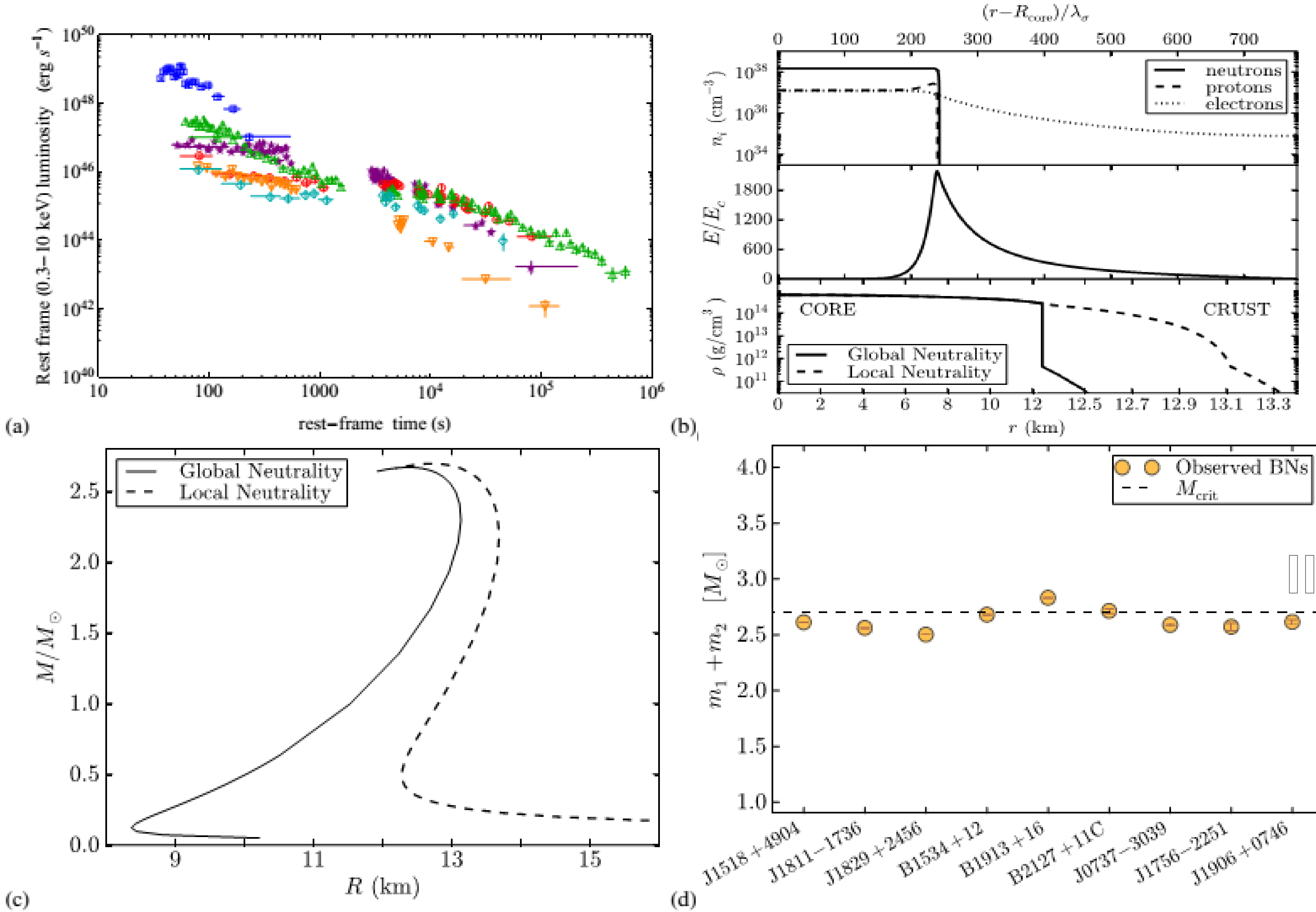

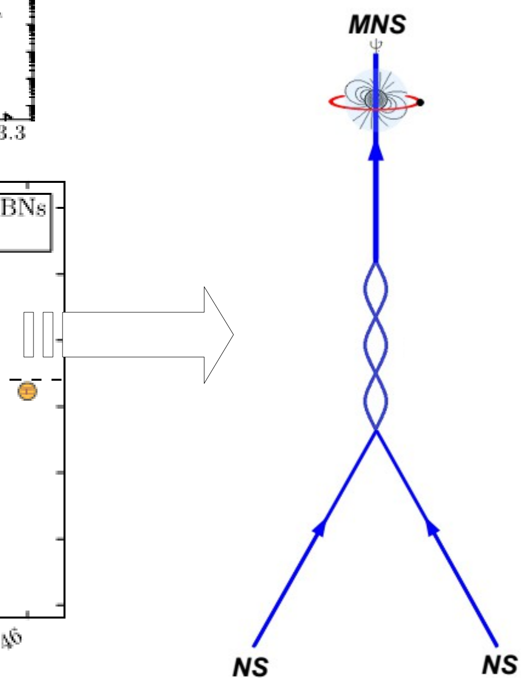

– **No BH formation;**

– **No GeV emission;**

– **$E_{iso}<10^{52}$ erg explained by $\nu\nu\rightarrow e^{+}e^{-}$ process [14,40–41].**

[40] Salmonson, J. D., & Wilson, J. R. 2002, ApJ, 578, 310

[41] Rosswog, S., Ramirez-Ruiz, E., & Davies, M. B. 2003, MNRAS, 345, 1077

The authentic short GRBs (S-GRBs) [33]

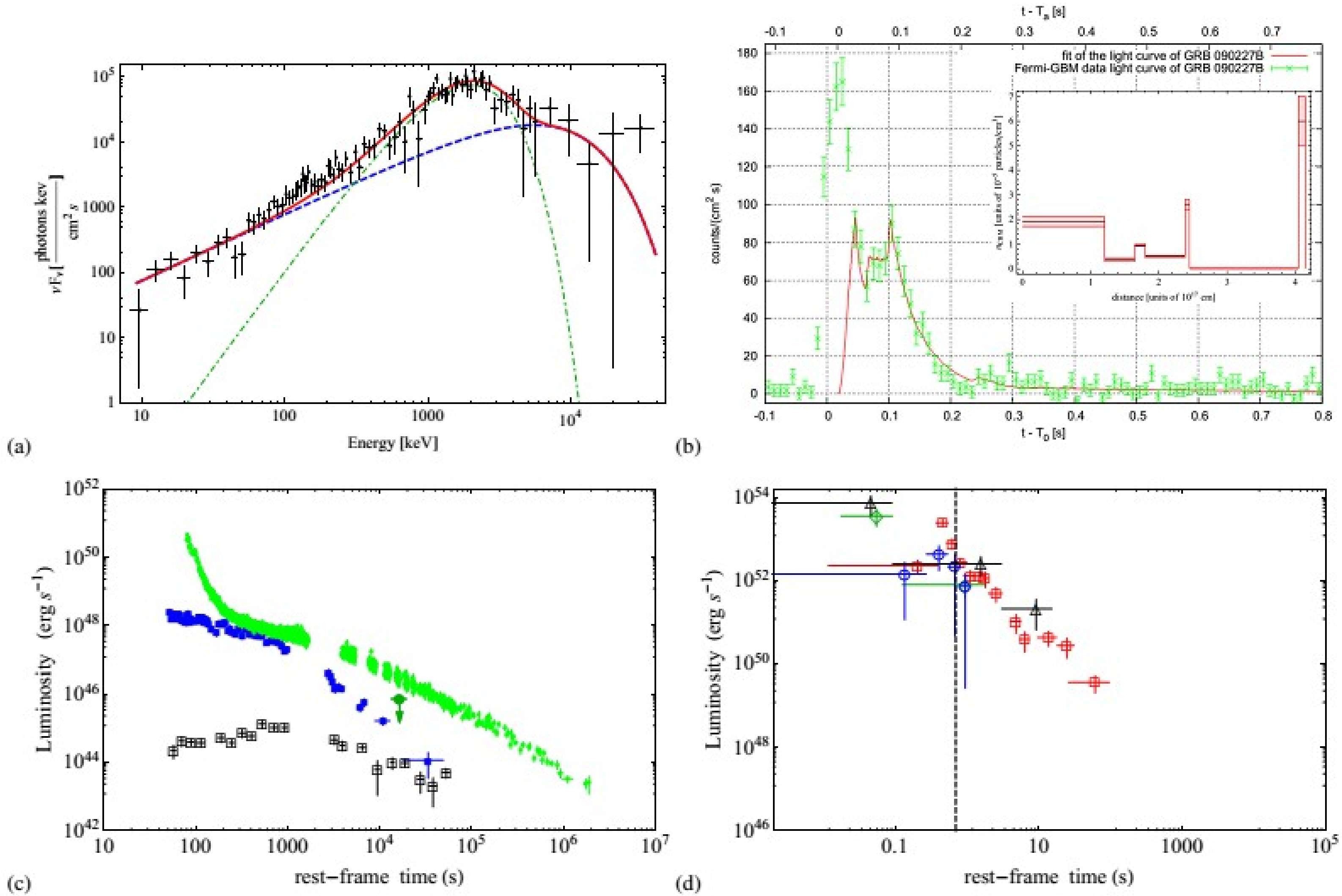

– **BH formation;**

– **GeV emission;**

– **E_{iso}>10^{52} erg explained by the collapse into a BH and the GRB emission [30,42].**

[42] Muccino, M., Ruffini, R., Bianco, C. L., Izzo, L., & Penacchioni, A. V. 2013, ApJ, 763, 125

The authentic short GRBs (S-GRBs) [33]

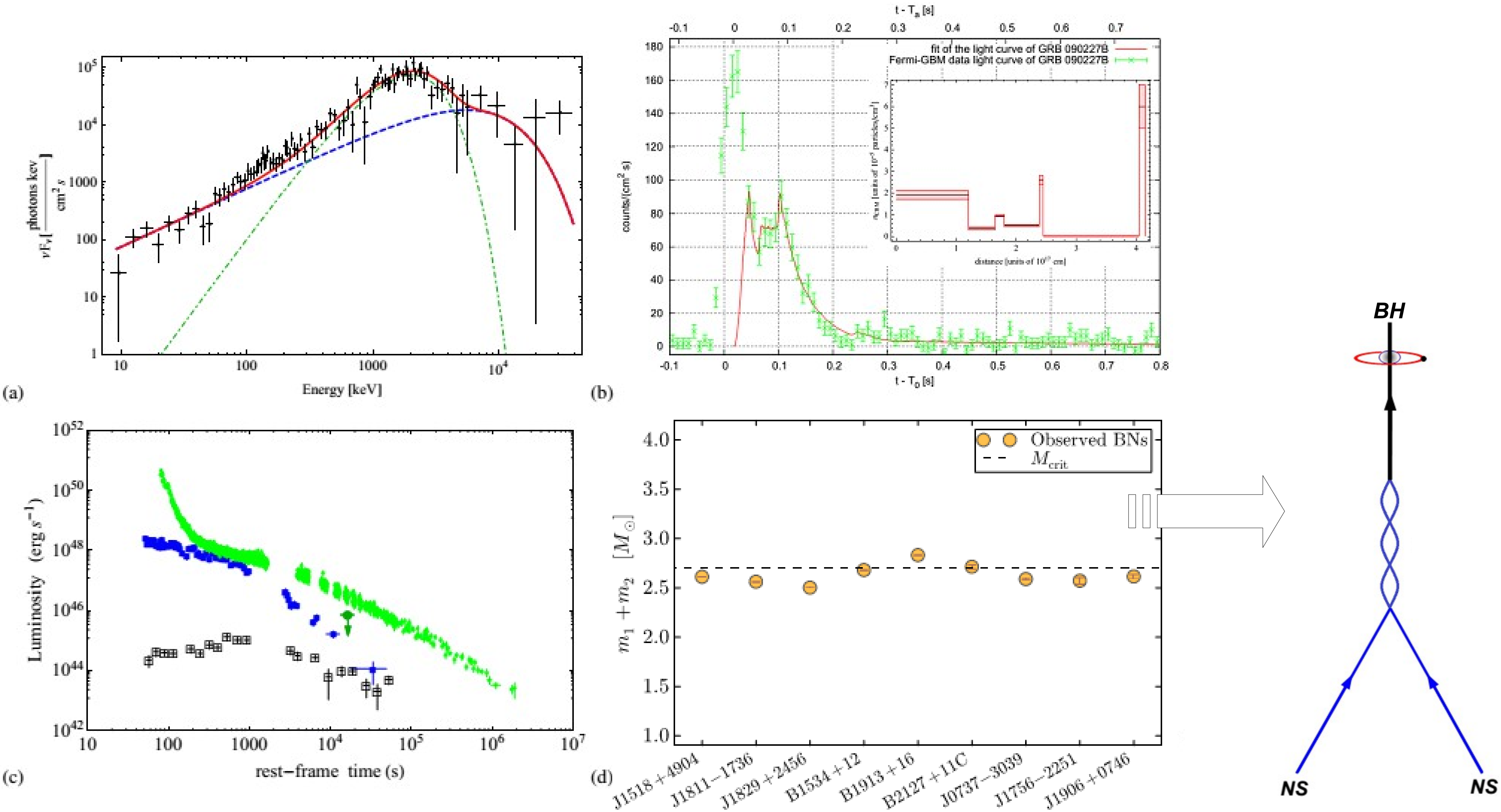

Also for S-GRBs we proposed that the BH formation is proven by its activity which consists in the GeV emission [30].

$E_{p,i}$-E_{iso} relations for short and long GRBs (3)

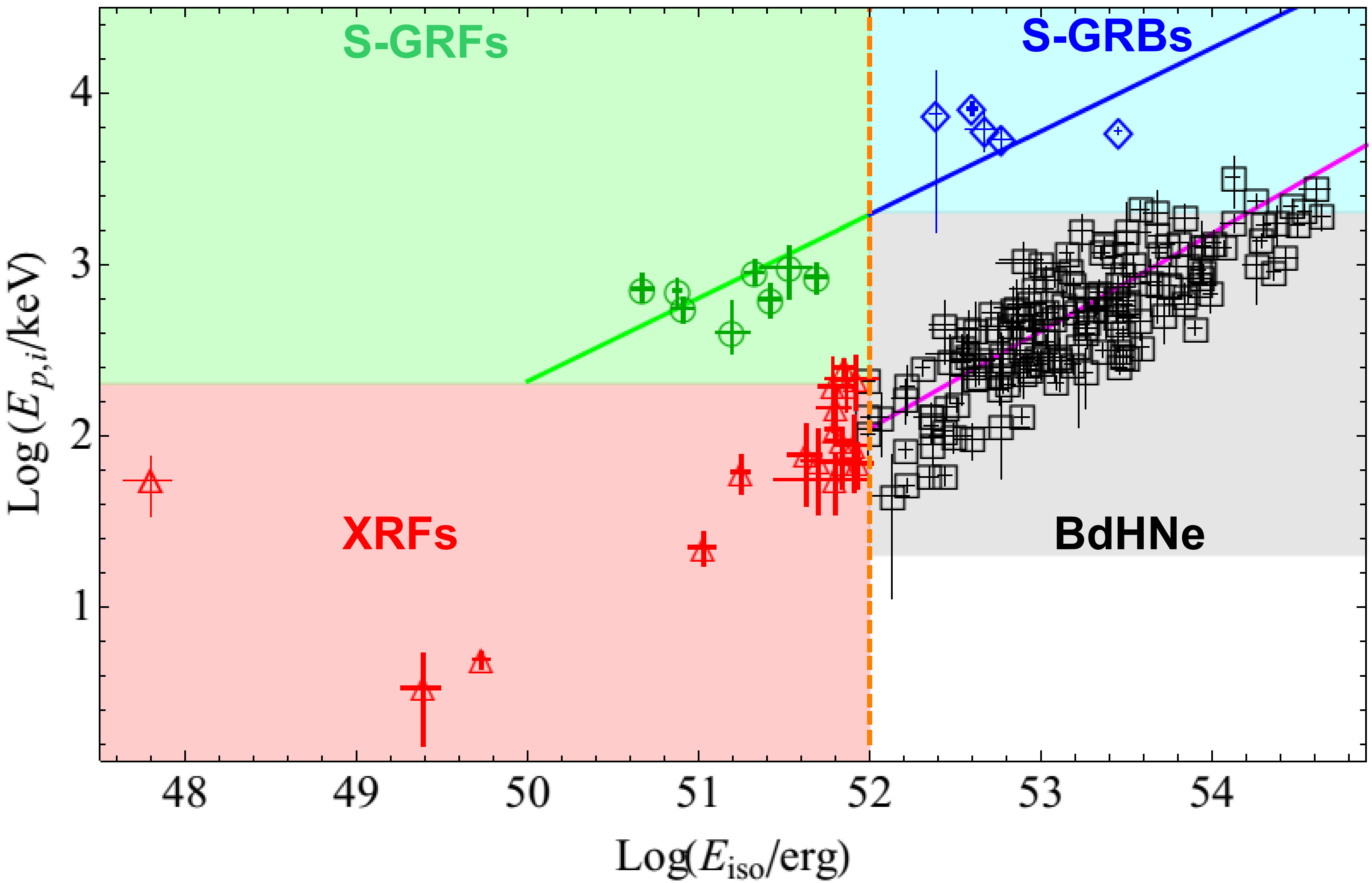

[28] Zhang, F.-W., Shao, L., Yan, J.-Z., & Wei, D.-M. 2012, ApJ, 750, 88.

[29] Calderone, G., Ghirlanda, G., Ghisellini, G., et al. 2015, MNRAS, 448, 403.

[30] Ruffini, R., Muccino, M., Kovacevic, M., et al. 2015, ApJ, 808, 190

[31] Amati, L., & Della Valle, M. 2013, International Journal of Modern Physics

The DS-GRFs [33]

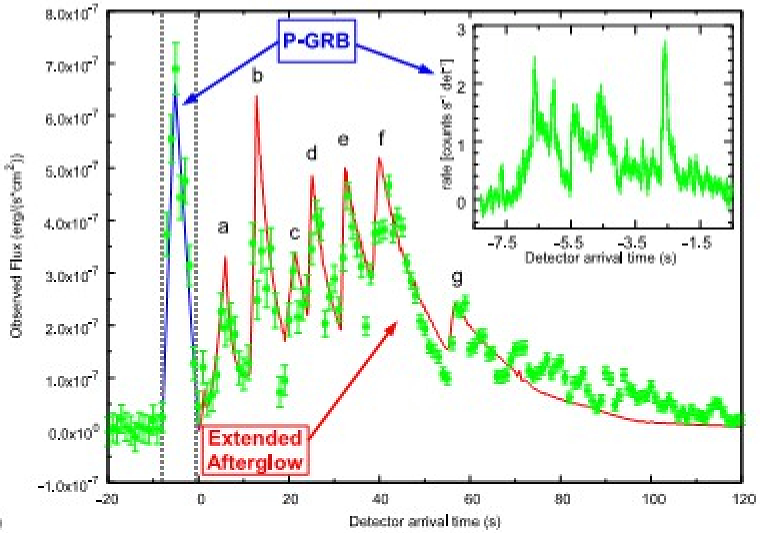

(a)

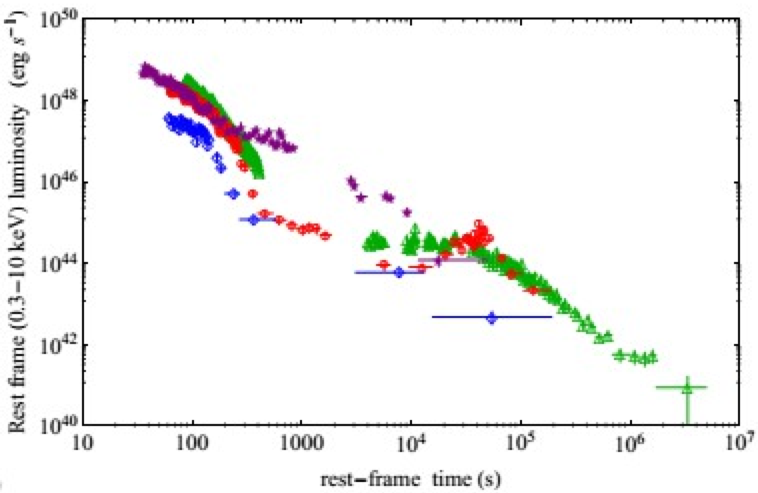

(b)

The DS-GRFs [33]

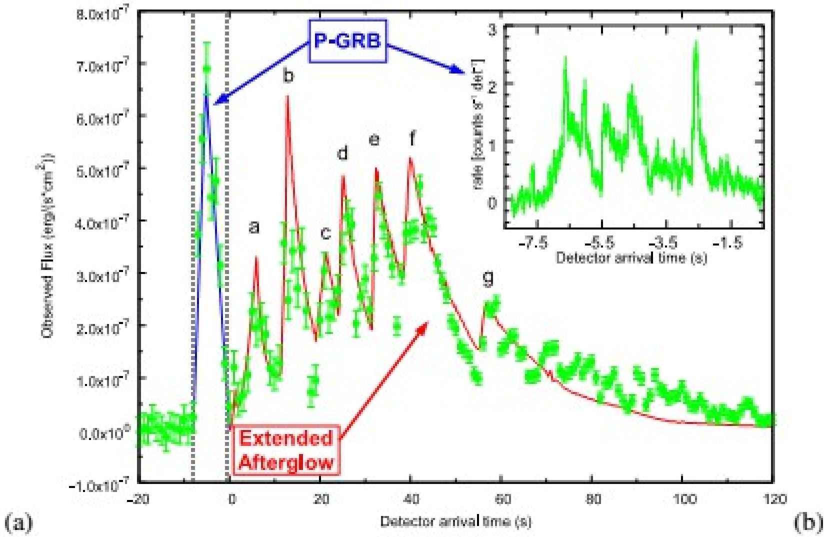

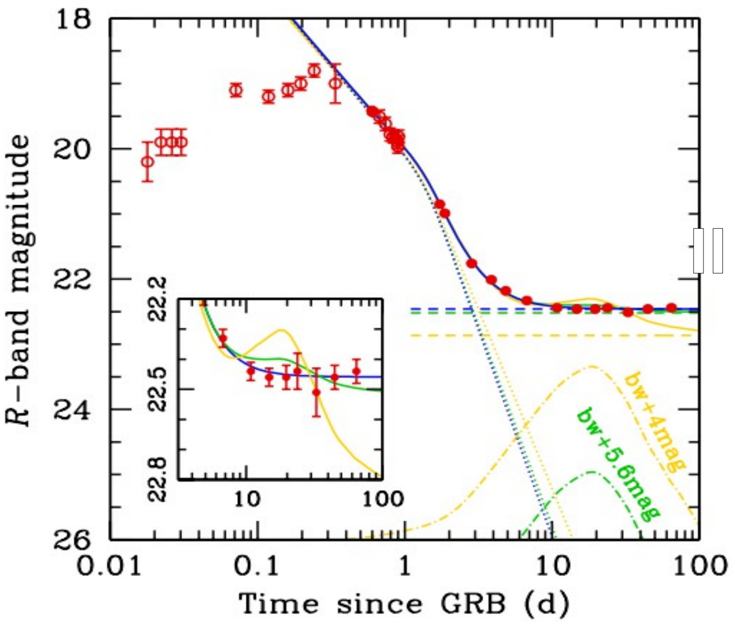

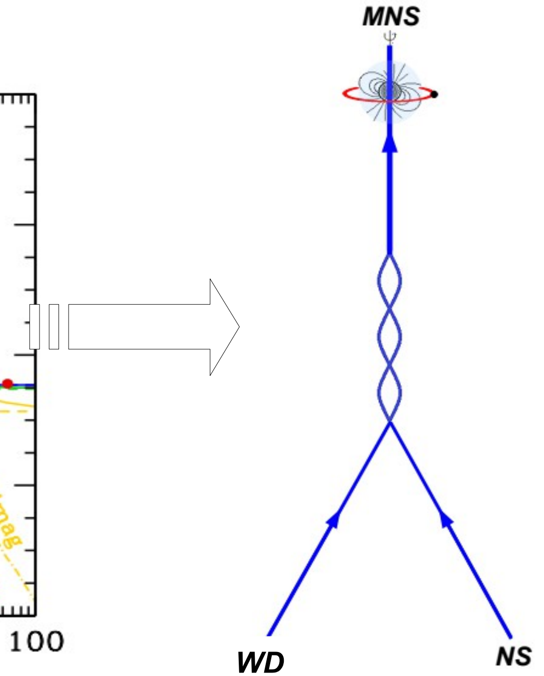

The DS-GRFs [33]

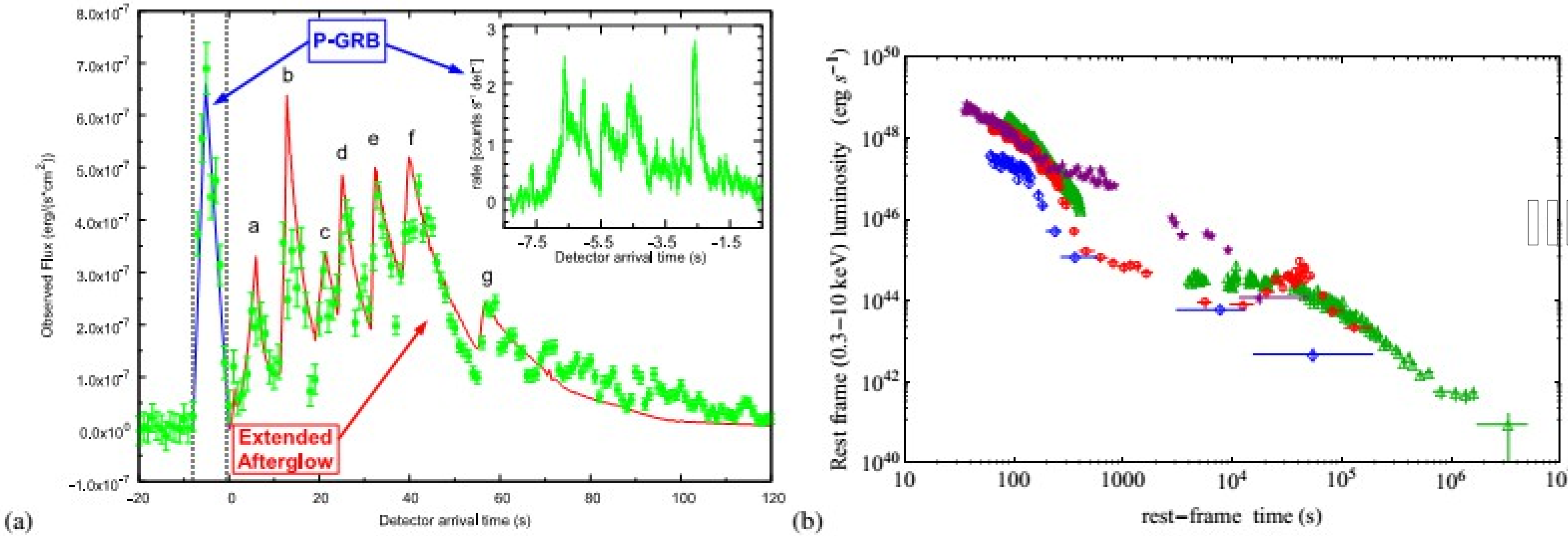

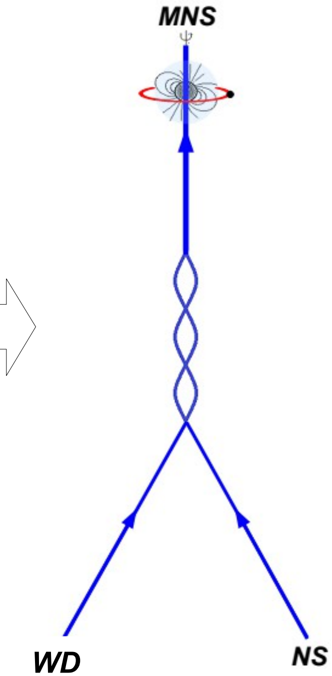

The ultrashort GRBs (U-GRBs) [33]

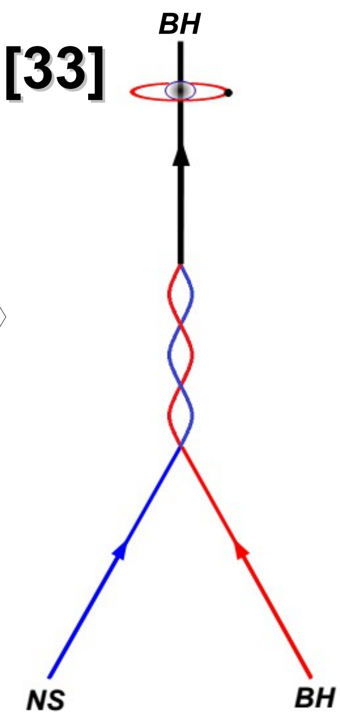

U-GRBs originate from the NS-BH binaries produced in the BdHNe and nearly 100% of these binaries remain bound [43]. The lack of any observed source to date is mainly due to the extremely short duration of these systems.

[43] Fryer, C. L., Oliveira, F. G., Rueda, J. A., & Ruffini, R. 2015, Physical Review Letters, 115, 231102.

$E_{p,i}$-E_{iso} relations for short and long GRBs (4)

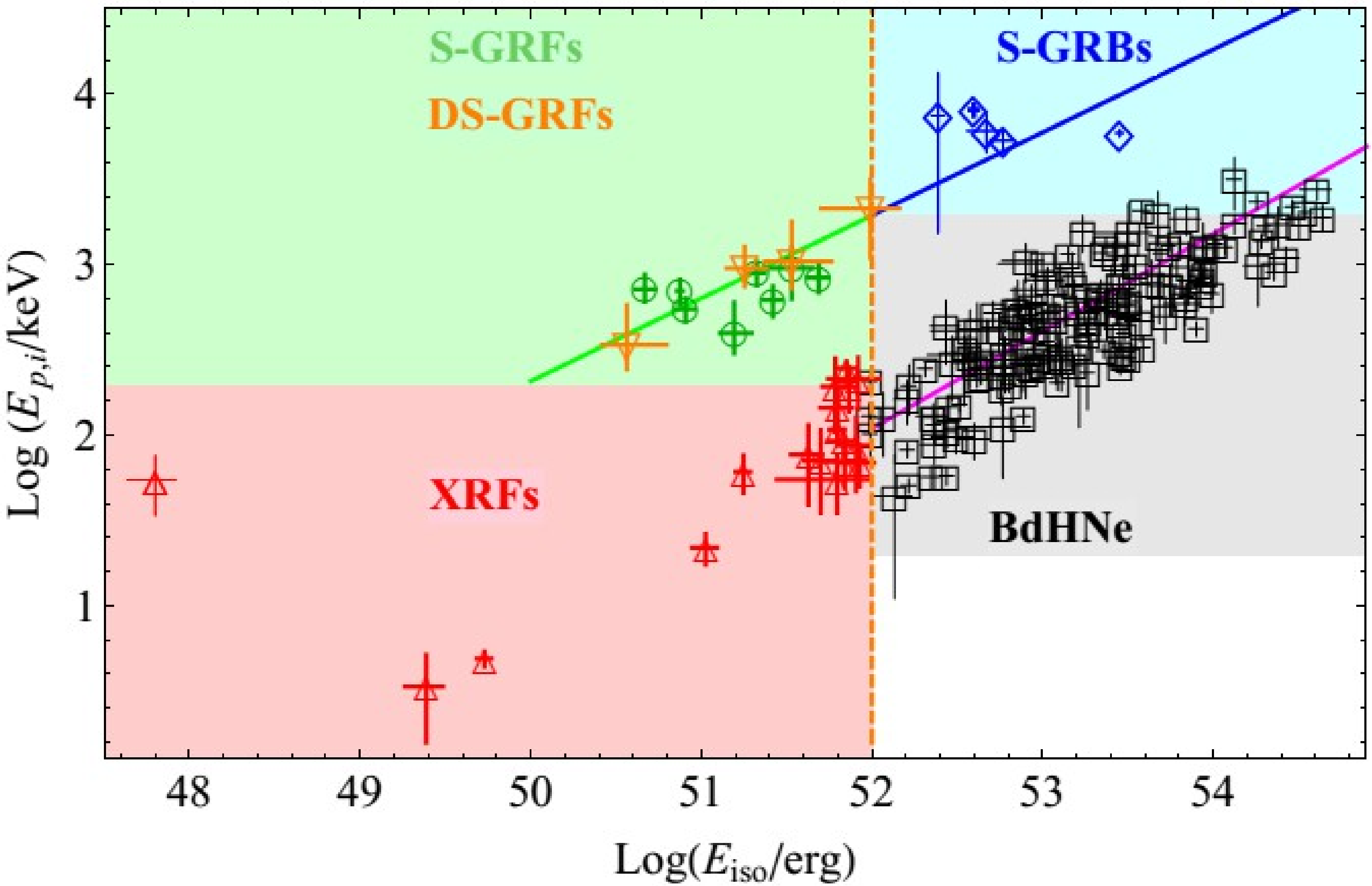

[28] Zhang, F.-W., Shao, L., Yan, J.-Z., & Wei, D.-M. 2012, ApJ, 750, 88.
[29] Calderone, G., Ghirlanda, G., Ghisellini, G., et al. 2015, MNRAS, 448, 403.
[30] Ruffini, R., Muccino, M., Kovacevic, M., et al. 2015, ApJ, 808, 190
[31] Amati, L., & Della Valle, M. 2013, International Journal of Modern Physics
[33] Ruffini, R., Rueda, J.A., Muccino, M., et al. 2016, arXiv:1602.02732

Rate of occurrence of our flash and burst sub-classes

Local rate estimates

Taking into account the observational constraints, i.e., the detector solid angle coverage of the sky and sensitivities, which define a maximum volume of observation depending on the intrinsic luminosity of the sources, we compute the local rates following Ref. [44]

$$\rho_0 \simeq \sum_i \sum_{\log L_{\rm min}}^{\log L_{\rm max}} \frac{4\pi}{\Omega_i T_i} \frac{1}{\ln 10} \frac{1}{g(L)} \frac{\Delta N_i}{\Delta \log L} \frac{\Delta L}{L} ,$$

where $g(L) = \int_0^{z_{\rm max}(L)} \frac{f(z)}{1+z} \frac{dV(z)}{dz} dz$ **and** $\frac{dV(z)}{dz} = \frac{c}{H_0} \frac{4\pi d_L^2}{(1+z)^2[\Omega_M(1+z)^3 + \Omega_\Lambda]^{1/2}}$

RESULTS [45]

- **XRFs:** $\rho_0 = 100^{+45}_{-34} \mathrm{Gpc}^{-3}\ \mathrm{y}^{-1}$
- **BdHNe: (U-GRBs)** $\rho_0 = 0.77^{+0.09}_{-0.08}\ \mathrm{Gpc}^{-3}\ \mathrm{y}^{-1}$
- **S-GRFs:** $\rho_0 = 3.6^{+1.4}_{-1.0}\ \mathrm{Gpc}^{-3}\ \mathrm{y}^{-1}$
- **S-GRBs:** $\rho_0 = \left(1.9^{+1.8}_{-1.1}\right) \times 10^{-3}\ \mathrm{Gpc}^{-3}\ \mathrm{y}^{-1}$
- **DS-GRFs:** $\rho_0 = 1.02^{+0.71}_{-0.46}\ \mathrm{Gpc}^{-3}\ \mathrm{y}^{-1}$

[44] Sun, H., Zhang, B., & Li, Z. 2015, ApJ, 812, 33
[45] Ruffini R., Rueda J. A., Muccino M., et al. 2016, arXiv:1602.02732

Local rate estimates

Taking into account the observational constraints, i.e., the detector solid angle coverage of the sky and sensitivities, which define a maximum volume of observation depending on the intrinsic luminosity of the sources, we compute the local rates following Ref. [44]

$$\rho_0 \simeq \sum_i \sum_{\log L_{\rm min}}^{\log L_{\rm max}} \frac{4\pi}{\Omega_i T_i} \frac{1}{\ln 10} \frac{1}{g(L)} \frac{\Delta N_i}{\Delta \log L} \frac{\Delta L}{L} ,$$

where $g(L) = \int_0^{z_{\rm max}(L)} \frac{f(z)}{1+z} \frac{dV(z)}{dz} dz$ **and** $\frac{dV(z)}{dz} = \frac{c}{H_0} \frac{4\pi d_L^2}{(1+z)^2[\Omega_M(1+z)^3+\Omega_\Lambda]^{1/2}}$

RESULTS [45]		**LITERATURE**
– XRFs:	$\rho_0 = 100^{+45}_{-34} \mathrm{Gpc}^{-3}\ \mathrm{y}^{-1}$	$\rightarrow$ 164^{+98}_{-65} $\mathbf{Gpc^{-3}\ y^{-1}}$ **[44]**
– BdHNe: (U-GRBs)	$\rho_0 = 0.77^{+0.09}_{-0.08}\ \mathrm{Gpc}^{-3}\ \mathrm{y}^{-1}$	
– S-GRFs:	$\rho_0 = 3.6^{+1.4}_{-1.0}\ \mathrm{Gpc}^{-3}\ \mathrm{y}^{-1}$	
– S-GRBs:	$\rho_0 = \left(1.9^{+1.8}_{-1.1}\right) \times 10^{-3}\ \mathrm{Gpc}^{-3}\ \mathrm{y}^{-1}$	
– DS-GRFs:	$\rho_0 = 1.02^{+0.71}_{-0.46}\ \mathrm{Gpc}^{-3}\ \mathrm{y}^{-1}$	

[44] Sun, H., Zhang, B., & Li, Z. 2015, ApJ, 812, 33
[45] Ruffini R., Rueda J. A., Muccino M., et al. 2016, arXiv:1602.02732

Local rate estimates

Taking into account the observational constraints, i.e., the detector solid angle coverage of the sky and sensitivities, which define a maximum volume of observation depending on the intrinsic luminosity of the sources, we compute the local rates following Ref. [44]

$$\rho_0 \simeq \sum_i \sum_{\log L_{\rm min}}^{\log L_{\rm max}} \frac{4\pi}{\Omega_i T_i} \frac{1}{\ln 10} \frac{1}{g(L)} \frac{\Delta N_i}{\Delta \log L} \frac{\Delta L}{L} ,$$

where $$g(L) = \int_0^{z_{\rm max}(L)} \frac{f(z)}{1+z} \frac{dV(z)}{dz} dz$$ **and** $$\frac{dV(z)}{dz} = \frac{c}{H_0} \frac{4\pi d_L^2}{(1+z)^2[\Omega_M(1+z)^3 + \Omega_\Lambda]^{1/2}}$$

RESULTS [45]		LITERATURE	
– XRFs:	$\rho_0 = 100^{+45}_{-34} \mathrm{Gpc}^{-3}\ \mathrm{y}^{-1}$	$164^{+98}_{-65} \mathbf{Gpc^{-3}\ y^{-1}}$	[44]
– BdHNe: (U-GRBs)	$\rho_0 = 0.77^{+0.09}_{-0.08}\ \mathrm{Gpc}^{-3}\ \mathrm{y}^{-1}$	$1.3^{+0.6}_{-0.7}\ \mathbf{Gpc^{-3}\ y^{-1}}$	[46]
		$0.8^{+0.1}_{-0.1}\ \mathbf{Gpc^{-3}\ y^{-1}}$	[44]
– S-GRFs:	$\rho_0 = 3.6^{+1.4}_{-1.0}\ \mathrm{Gpc}^{-3}\ \mathrm{y}^{-1}$		
– S-GRBs:	$\rho_0 = \left(1.9^{+1.8}_{-1.1}\right) \times 10^{-3}\ \mathrm{Gpc}^{-3}\ \mathrm{y}^{-1}$		
– DS-GRFs:	$\rho_0 = 1.02^{+0.71}_{-0.46}\ \mathrm{Gpc}^{-3}\ \mathrm{y}^{-1}$		

[44] Sun, H., Zhang, B., & Li, Z. 2015, ApJ, 812, 33
[45] Ruffini R., Rueda J. A., Muccino M., et al. 2016, arXiv:1602.02732
[46] Wanderman, D., & Piran, T. 2010, MNRAS, 406, 1944

Local rate estimates

Taking into account the observational constraints, i.e., the detector solid angle coverage of the sky and sensitivities, which define a maximum volume of observation depending on the intrinsic luminosity of the sources, we compute the local rates following Ref. [44]

$$\rho_0 \simeq \sum_i \sum_{\log L_{\rm min}}^{\log L_{\rm max}} \frac{4\pi}{\Omega_i T_i} \frac{1}{\ln 10} \frac{1}{g(L)} \frac{\Delta N_i}{\Delta \log L} \frac{\Delta L}{L} ,$$

where $g(L) = \int_0^{z_{\rm max}(L)} \frac{f(z)}{1+z} \frac{dV(z)}{dz} dz$ **and** $\frac{dV(z)}{dz} = \frac{c}{H_0} \frac{4\pi d_L^2}{(1+z)^2[\Omega_M(1+z)^3 + \Omega_\Lambda]^{1/2}}$

RESULTS [45]

- **XRFs:** $\rho_0 = 100^{+45}_{-34} \mathrm{Gpc}^{-3}\ \mathrm{y}^{-1}$
- **BdHNe: (U-GRBs)** $\rho_0 = 0.77^{+0.09}_{-0.08}\ \mathrm{Gpc}^{-3}\ \mathrm{y}^{-1}$
- **S-GRFs:** $\rho_0 = 3.6^{+1.4}_{-1.0}\ \mathrm{Gpc}^{-3}\ \mathrm{y}^{-1}$
- **S-GRBs:** $\rho_0 = \left(1.9^{+1.8}_{-1.1}\right) \times 10^{-3}\ \mathrm{Gpc}^{-3}\ \mathrm{y}^{-1}$
- **DS-GRFs:** $\rho_0 = 1.02^{+0.71}_{-0.46}\ \mathrm{Gpc}^{-3}\ \mathrm{y}^{-1}$

LITERATURE

- $164^{+98}_{-65}\,\mathbf{Gpc^{-3}\ y^{-1}}$ [44]
- $1.3^{+0.6}_{-0.7}\ \mathbf{Gpc^{-3}\ y^{-1}}$ [46]
- $0.8^{+0.1}_{-0.1}\ \mathbf{Gpc^{-3}\ y^{-1}}$ [44]
- $4.1^{+2.3}_{-1.9}\ \mathbf{Gpc^{-3}\ y^{-1}}$ [47]
- $4.2^{+1.3}_{-1.0}, 3.9^{+1.2}_{-0.9}, 7.1^{+2.2}_{-1.7}\ \mathbf{Gpc^{-3}\ y^{-1}}$ [44]

[44] Sun, H., Zhang, B., & Li, Z. 2015, ApJ, 812, 33
[45] Wanderman, D., & Piran, T. 2010, MNRAS, 406, 1944
[46] Wanderman, D., & Piran, T. 2010, MNRAS, 406, 1944
[47] Wanderman, D., & Piran, T. 2015, MNRAS, 448, 3026

Local rate estimates

Taking into account the observational constraints, i.e., the detector solid angle coverage of the sky and sensitivities, which define a maximum volume of observation depending on the intrinsic luminosity of the sources, we compute the local rates following Ref. [44]

$$\rho_0 \simeq \sum_i \sum_{\log L_{\rm min}}^{\log L_{\rm max}} \frac{4\pi}{\Omega_i T_i} \frac{1}{\ln 10} \frac{1}{g(L)} \frac{\Delta N_i}{\Delta \log L} \frac{\Delta L}{L} ,$$

where $g(L) = \int_0^{z_{\rm max}(L)} \frac{f(z)}{1+z} \frac{dV(z)}{dz} dz$ **and** $\frac{dV(z)}{dz} = \frac{c}{H_0} \frac{4\pi d_L^2}{(1+z)^2[\Omega_M(1+z)^3 + \Omega_\Lambda]^{1/2}}$

RESULTS [45]		LITERATURE	
– XRFs:	$\rho_0 = 100^{+45}_{-34} \mathrm{Gpc}^{-3}\ \mathrm{y}^{-1}$	$164^{+98}_{-65} \mathbf{Gpc}^{-3}\ \mathbf{y}^{-1}$	[44]
– BdHNe: (U-GRBs)	$\rho_0 = 0.77^{+0.09}_{-0.08}\ \mathrm{Gpc}^{-3}\ \mathrm{y}^{-1}$	$1.3^{+0.6}_{-0.7}\ \mathbf{Gpc}^{-3}\ \mathbf{y}^{-1}$	[46]
		$0.8^{+0.1}_{-0.1}\ \mathbf{Gpc}^{-3}\ \mathbf{y}^{-1}$	[44]
– S-GRFs:	$\rho_0 = 3.6^{+1.4}_{-1.0}\ \mathrm{Gpc}^{-3}\ \mathrm{y}^{-1}$	$4.1^{+2.3}_{-1.9}\ \mathbf{Gpc}^{-3}\ \mathbf{y}^{-1}$	[47]
– S-GRBs:	$\rho_0 = \left(1.9^{+1.8}_{-1.1}\right) \times 10^{-3}\ \mathrm{Gpc}^{-3}\ \mathrm{y}^{-1}$	$4.2^{+1.3}_{-1.0}, 3.9^{+1.2}_{-0.9}, 7.1^{+2.2}_{-1.7}\ \mathbf{Gpc}^{-3}\ \mathbf{y}^{-1}$	[44]
– DS-GRFs:	$\rho_0 = 1.02^{+0.71}_{-0.46}\ \mathrm{Gpc}^{-3}\ \mathrm{y}^{-1}$ **NEW!**		

[44] Sun, H., Zhang, B., & Li, Z. 2015, ApJ, 812, 33
[45] Wanderman, D., & Piran, T. 2010, MNRAS, 406, 1944
[46] Wanderman, D., & Piran, T. 2010, MNRAS, 406, 1944
[47] Wanderman, D., & Piran, T. 2015, MNRAS, 448, 3026

Redshift evolution of the rates

We use in Ref. [45] the same method of Ref. [44] in different redshift bins

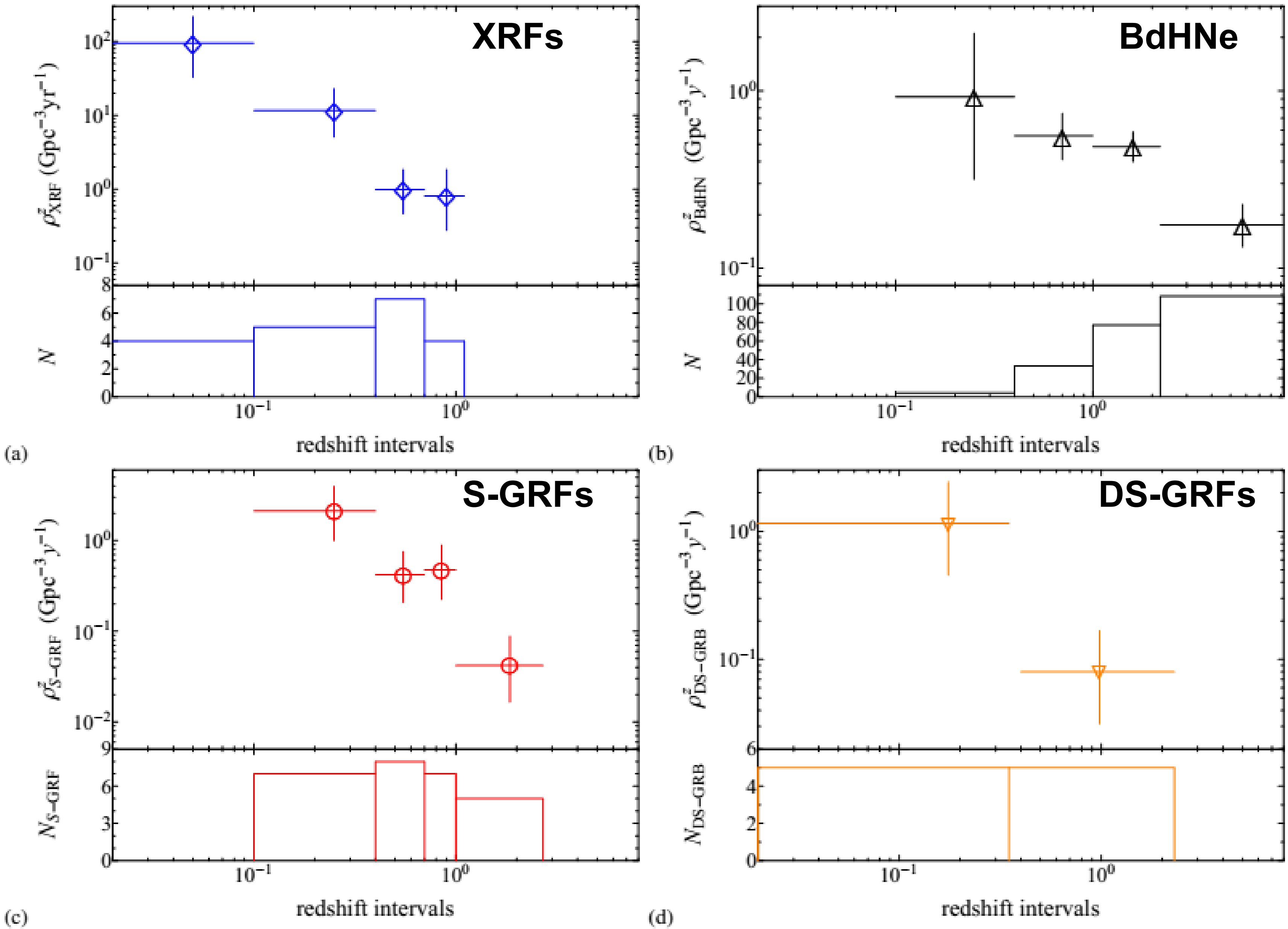

[44] Sun, H., Zhang, B., & Li, Z. 2015, ApJ, 812, 33
[45] Ruffini R., Rueda J. A., Muccino M., et al. 2016, arXiv:1602.02732

Redshift evolution of the rates

How do these rates compare each other?

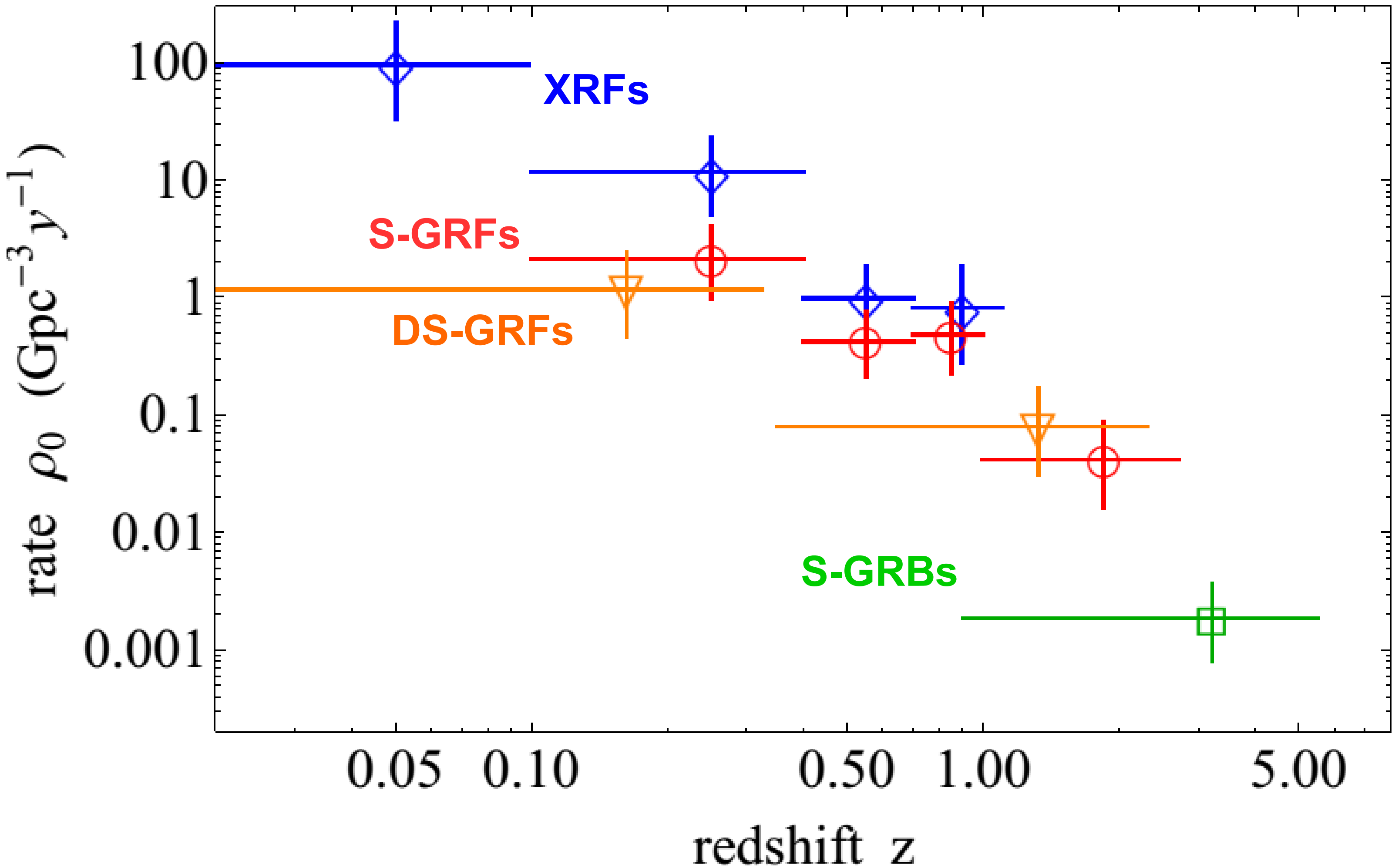

GRB rates vs aLIGO detections

How many aLIGO detections are expected from the inferred GRB local rates?

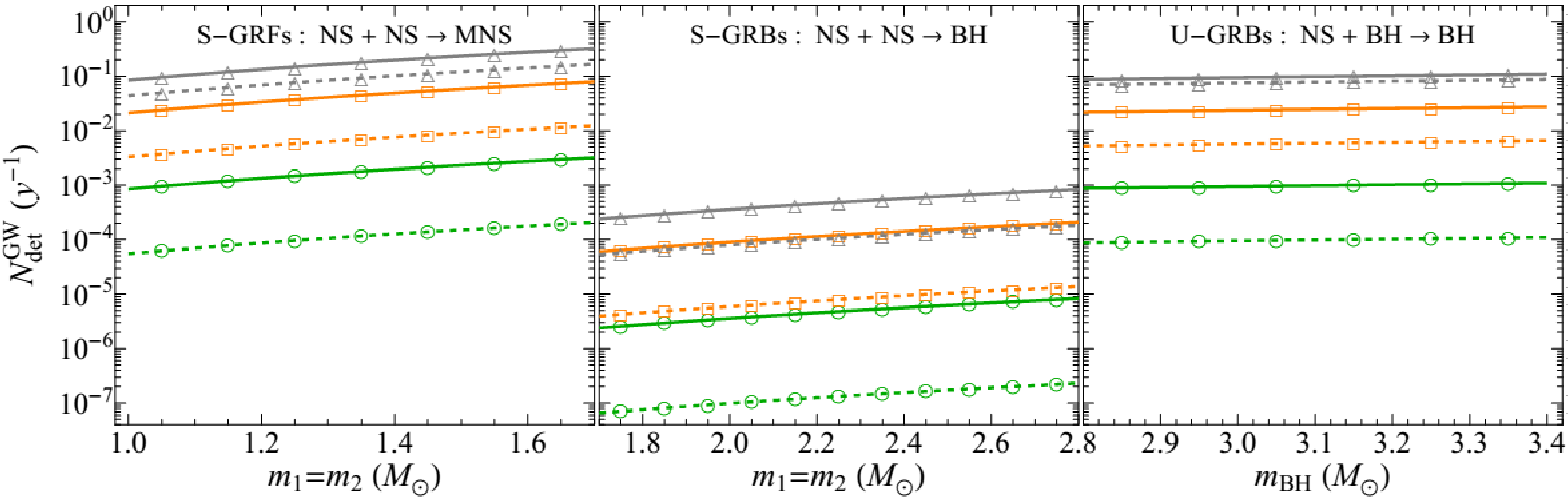

in-states	out-states	$E_{\rm p,i}$ (MeV)	$E_{\rm iso}$ (erg)	$E_{\rm iso,X}$ (erg)	$E_{\rm iso,Gev}$ (erg)	$z_{\rm max}$	ρ_0 ($\rm Gpc^{-3}\ yr^{-1}$)	$\dot{N}_{\rm GRB}$ ($\rm yr^{-1}$)		$\dot{N}_{\rm GW}$
Subclass: **S-GRF**										$1.4{+}1.4\ M_\odot$
NS-NS	MNS	$\lesssim 2$	$\sim 10^{49}$–10^{52}	$\sim 10^{49}$–10^{51}	–	2.609	$3.6^{+1.4}_{-1.0}$	58–248	(2015)	0.1–2 $\rm kyr^{-1}$
									(2017/18)	8–49 $\rm kyr^{-1}$
									(2022)	102–196 $\rm kyr^{-1}$
Subclass: **S-GRB**										$2.0{+}2.0\ M_\odot$
NS-NS	BH	$\gtrsim 2$	$\sim 10^{52}$–10^{53}	$\lesssim 10^{51}$	$\sim 10^{52}$–10^{53}	5.52	$(1.9^{+1.8}_{-1.1}) \times 10^{-3}$	2–8	(2015)	0.1–4 $\rm Myr^{-1}$
									(2017/18)	6–90 $\rm Myr^{-1}$
									(2022)	80–360 $\rm Myr^{-1}$
Subclass: **U-GRB**										$1.5{+}3.0\ M_\odot$
NS-BH	BH	$\gtrsim 2$	$> 10^{52}$	–	–	–	$\gtrsim 0.77^{+0.09}_{-0.08}$	–	(2015)	$\gtrsim$ 0.09–0.9 $\rm kyr^{-1}$
									(2017/18)	$\gtrsim$ 6–24 $\rm kyr^{-1}$
									(2022)	$\gtrsim$ 76–95 $\rm kyr^{-1}$

Conclusions (1)

	Long bursts		Short bursts			Hybrid long/short bursts
Progenitor	CO_{core}–NS		NS–NS		NS–BH	NS–WD
SN	always		never		never	never
	$E_{iso}<10^{52}$ erg	$E_{iso}>10^{52}$ erg	$E_{iso}<10^{52}$ erg	$E_{iso}>10^{52}$ erg	$E_{iso}\gtrsim10^{54}$ erg	$E_{iso}<10^{52}$ erg
Sub-class	XRF	BdHN	S-GRF	S-GRB	U-GRB	DS-GRF
BH	NO	YES	NO	YES	YES	NO
Hard spectrum	NO ($E_{p,i}$ <200 keV)	YES ($E_{p,i}$ >200 keV)	YES ($E_{p,i}$ <2 MeV)	YES ($E_{p,i}$ >2 MeV)	YES ($E_{p,i}$ >2 MeV)	YES ($E_{p,i}$ <2 MeV)
X-ray	YES (no scaling)	YES (scaling)	YES (no scaling)	YES (no scaling)	YES (no scaling)	YES (no scaling)
GeV	NO	YES	NO	YES	YES	NO
Outcome	NS–NS	NS–BH	MNS	BH	BH	MNS
Rate ($Gpc^{-3}y^{-1}$)	66–145	0.69–0.86	2.6–4.9	$(0.8–3.7)\times10^{-3}$	0.69–0.86	0.52–1.73

Conclusions (2)

in-states	out-states	$E_{\rm p,i}$ (MeV)	$E_{\rm iso}$ (erg)	$E_{\rm iso,X}$ (erg)	$E_{\rm iso,Gev}$ (erg)	$z_{\rm max}$	ρ_0 ($\rm Gpc^{-3}\ yr^{-1}$)	$\dot{N}_{\rm GRB}$ ($\rm yr^{-1}$)		$\dot{N}_{\rm GW}$
Subclass: **S-GRF**										1.4+1.4 $M_\odot$
NS-NS	MNS	$\lesssim 2$	$\sim 10^{49}$–10^{52}	$\sim 10^{49}$–10^{51}	–	2.609	$3.6^{+1.4}_{-1.0}$	58–248	(2015)	0.1–2 $\rm kyr^{-1}$
									(2017/18)	8–49 $\rm kyr^{-1}$
									(2022)	102–196 $\rm kyr^{-1}$
Subclass: **S-GRB**										2.0+2.0 $M_\odot$
NS-NS	BH	$\gtrsim 2$	$\sim 10^{52}$–10^{53}	$\lesssim 10^{51}$	$\sim 10^{52}$–10^{53}	5.52	$(1.9^{+1.8}_{-1.1}) \times 10^{-3}$	2–8	(2015)	0.1–4 $\rm Myr^{-1}$
									(2017/18)	6–90 $\rm Myr^{-1}$
									(2022)	80–360 $\rm Myr^{-1}$
Subclass: **U-GRB**										1.5+3.0 $M_\odot$
NS-BH	BH	$\gtrsim 2$	$> 10^{52}$	–	–	–	$\gtrsim 0.77^{+0.09}_{-0.08}$	–	(2015)	$\gtrsim$ 0.09–0.9 $\rm kyr^{-1}$
									(2017/18)	$\gtrsim$ 6–24 $\rm kyr^{-1}$
									(2022)	$\gtrsim$ 76–95 $\rm kyr^{-1}$

Conclusions (3)

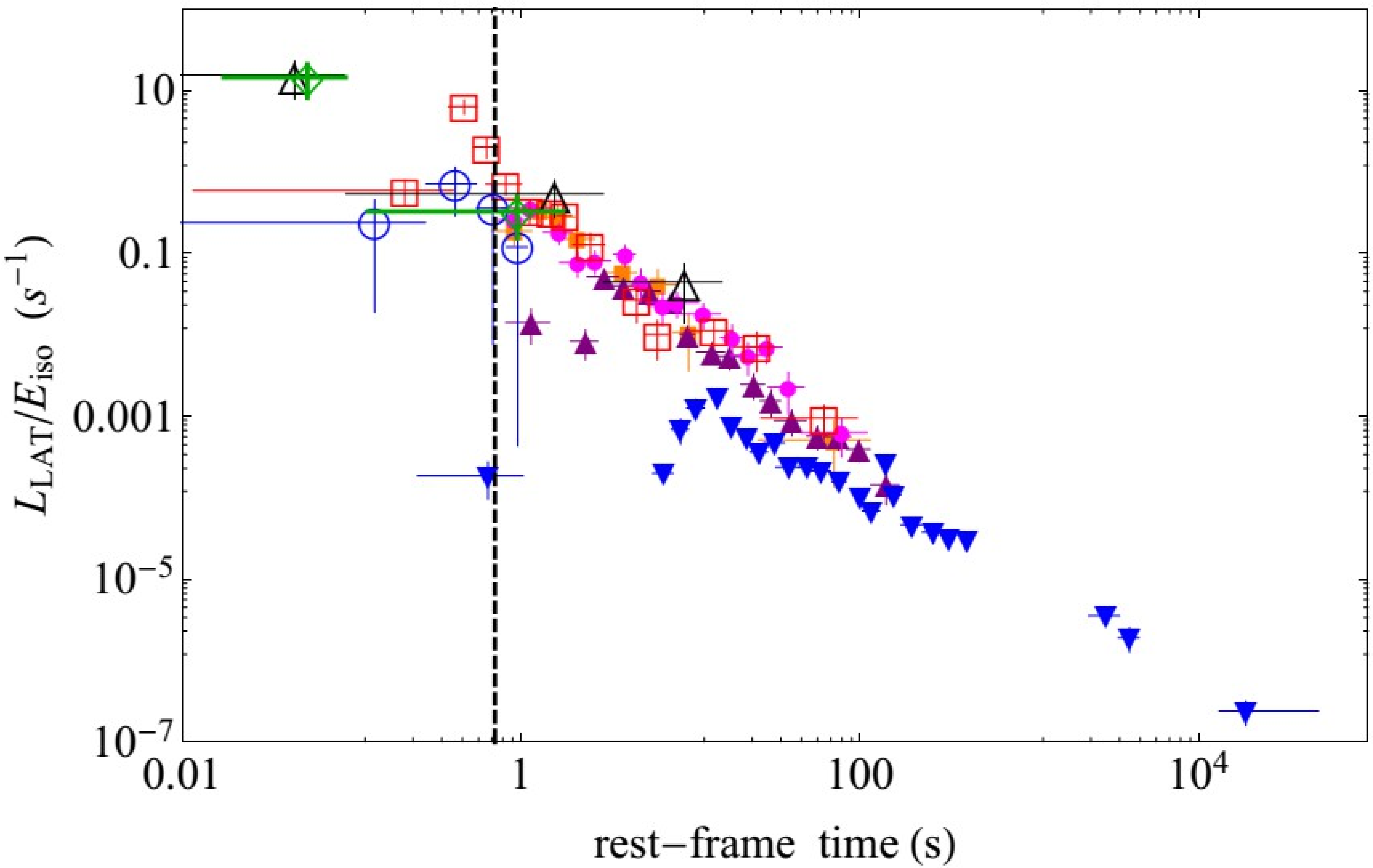

Thank you